# Approximation by Quad Meshes in Laguerre Geometry

Anthony Ramos-Cisneros[a,*], Mikhail Skopenkov[a] and Helmut Pottmann[b]

[a] *King Abdullah University of Science and Technology, Thuwal, 23955-6900, Makkah, Saudi Arabia*
[b] *Institute of Discrete Mathematics and Geometry, Vienna University of Technology, Vienna, 1040, Austria*

ARTICLE INFO

*Keywords*:
sphere mesh
Laguerre geometry
discrete differential geometry
sphere congruence
L-mesh
L-conjugacy

ABSTRACT

We study analogs of planar-quadrilateral meshes in Laguerre sphere geometry and the approximation of smooth surfaces by them. These new *Laguerre meshes* can be viewed as watertight surfaces formed by planar quadrilaterals , strips of right circular cones (representing the edges), and spherical panels. In the smooth limit, we get an analog of conjugate nets in Laguerre geometry, which we call *Laguerre conjugate nets* with respect to an attached sphere congruence. We introduce the notion of *Laguerre conjugate directions*, provide a method for computing them, and apply them to approximate surfaces by L-meshes with prescribed radii of spherical panels.

## 1. Introduction

The availability of spherical glass panels for cladding architectural skins has motivated recent research on meshes with spherical panels. This work aims at an extension of basic properties and results from discrete differential geometry on meshes with planar faces (Bobenko and Suris, 2008) towards their counterparts in sphere geometries. Initially, the focus has been on meshes in Möbius geometry (Kilian, Ramos-Cisneros, Müller and Pottmann, 2023; Ramos-Cisneros, Aikyn, Kilian, Pottmann and Müller, 2024), which are formed by spherical faces and circular edges, and on their application to computational design and approximation problems.

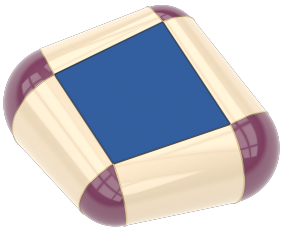

A study of their counterparts in Laguerre sphere geometry is not straightforward and a topic of our ongoing research. One can see these Laguerre meshes, shortly called *L-meshes*, as watertight surfaces that are formed by planar polygons, strips of right circular cones (representing the edges), and spherical panels (see see inset figure, Figs. 1 and 2). Here, conical panels are also useful in architecture due to their reduced manufacturing cost, a particular case of paneling freeform surfaces with developable pieces (Gavriil, Schiftner and Pottmann, 2019).

If an L-mesh closely approximates an underlying $C^2$ reference surface $f$, its appearance depends on the sign of the Gaussian curvature of $f$. In areas of positive curvature of $f$, the L-mesh is typically a $C^1$ surface, in contrast to their Möbius geometric counterparts, which are just $C^0$ surfaces. In negatively curved areas, the surface represented by an L-mesh still has continuous tangent planes, but is not regular anymore. Rather, the surface exhibits regression curves, the appearance of which is known from offset surfaces. This is not surprising, as offsetting is a special Laguerre transformation. More generally, applying a Laguerre transformation to a smooth L-mesh may result in the appearance of singularities in the point set.

The present paper deals with the *approximation of a given surface $f$ by a quad-L-mesh*, in which every planar and every spherical panel is surrounded by four conical patches in a "gingham" pattern (see, for example, Figs. 3 and 4). While we allow isolated combinatorial singularities, we focus on regions with square grid ($\mathbb{Z}^2$) combinatorics and call them *L-nets*. However, we want to *prescribe the sphere radii of the mesh spheres*. This may depend on the application. A natural choice can be spheres that are good local approximations of $f$.

Let us first look at a limit case where all spheres in an L-net have radius zero. Now, it is the same as a quad mesh with planar faces, called Q-net in discrete differential geometry. Such Q-nets are discrete counterparts of conjugate surface parameterizations (Bobenko and Suris, 2008) and this property is fundamental for solving the approximation problem (see e.g. (Liu, Pottmann, Wallner, Yang and Wang, 2006; Pottmann, Eigensatz, Vaxman and Wallner, 2015)).

*Corresponding author
anthony.cisneros@kaust.edu.sa (A. Ramos-Cisneros); mikhail.skopenkov@gmail.com (M. Skopenkov); pottmann@geometrie.tuwien.ac.at (H. Pottmann)
ORCID(s): 0000-0001-5430-6193 (A. Ramos-Cisneros); 0000-0003-2453-0009 (M. Skopenkov); 0000-0002-3195-9316 (H. Pottmann)

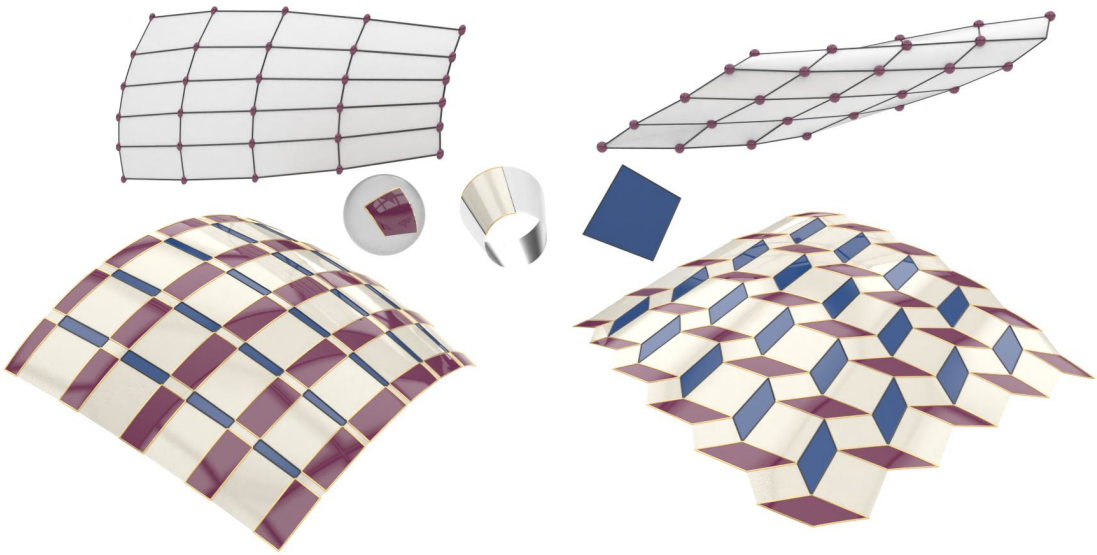

**Figure 1:** An L-mesh represents a smooth surface in positively curved areas, and consists of planar quads (blue), spherical panels bounded by circular arcs (red), and pieces of rotational cones (beige), viewed as its edges. For an L-mesh that is a discrete principal parameterization, the overall pattern is smooth (left), while in a more general case, one has a staircase pattern (right). The sphere centers (red) form a mesh (gray) with gradually curving discrete parameter lines (top row).

One cannot just apply numerical optimization to any initial quad mesh and push it towards an approximating Q-net. Rather, the edges of the initial mesh should follow the directions in a conjugate frame field of $f$.

Our problem has a similar structure, which led us to a generalization of the concept of conjugacy to a Laguerre geometric counterpart, which we call *L-conjugacy*. This allows us to follow a similar approximation approach for the present problem, where the sphere radii are prescribed. L-conjugacy is defined for a surface $f$ equipped with an attached sphere congruence, i.e., a 2-parameter family of spheres tangent to $f$. As we did not find such a concept in the literature, we first provide a thorough study and then apply it to the approximation.

## 1.1. Contributions and overview

The goal of the present research is the approximation of a given surface with positive Gaussian curvature by L-nets.

L-nets consist of smoothly joined planar, conical and spherical panels. For good approximation quality and other applications, we want to control the spheres through their radii. Hence, our L-nets approximate a surface $f$ that appears as an envelope of a two-parameter family of spheres.

After an introduction to basic concepts of Laguerre geometry and meshes in this sphere geometry (Sec. 2), we introduce L-nets, in the discrete and smooth version in Sec. 2.3 and 3, respectively. The control over the spheres through their radii amounts to the new concept of L-conjugate parameterizations of a surface with respect to an attached sphere congruence. We first derive the characterizing geometric properties and analytical representations of these parameterizations in the 4-dimensional Minkowski space (Sec. 3.1), and then turn to the Laguerre geometry in Euclidean 3-space (Sec. 3.2). Sec. 4 relates L-conjugacy to a dual viewpoint of surface theory that is based on dual curvature radii. The number of self-L-conjugate directions provides a classification of contact elements of surfaces (Sec. 4.1). In Sec. 4.2, we discuss L-asymptotic parameterizations and their relation to a Laguerre geometric formulation of principal symmetric parameterizations (Pellis, Wang, Kilian, Rist, Pottmann and Müller, 2020). L-conjugacy with respect to important particular attached sphere congruences is studied in Sec. 4.3. In Sec. 5, L-conjugacy serves for initialization of a numerical optimization algorithm which computes an L-net that approximates a given surface with control over its spheres. Various examples demonstrate the effectiveness of our approach and illustrate the design flexibility and the quality of the resulting L-nets. We conclude with computed examples demonstrating our algorithm and pointers to future research in Sec. 6.

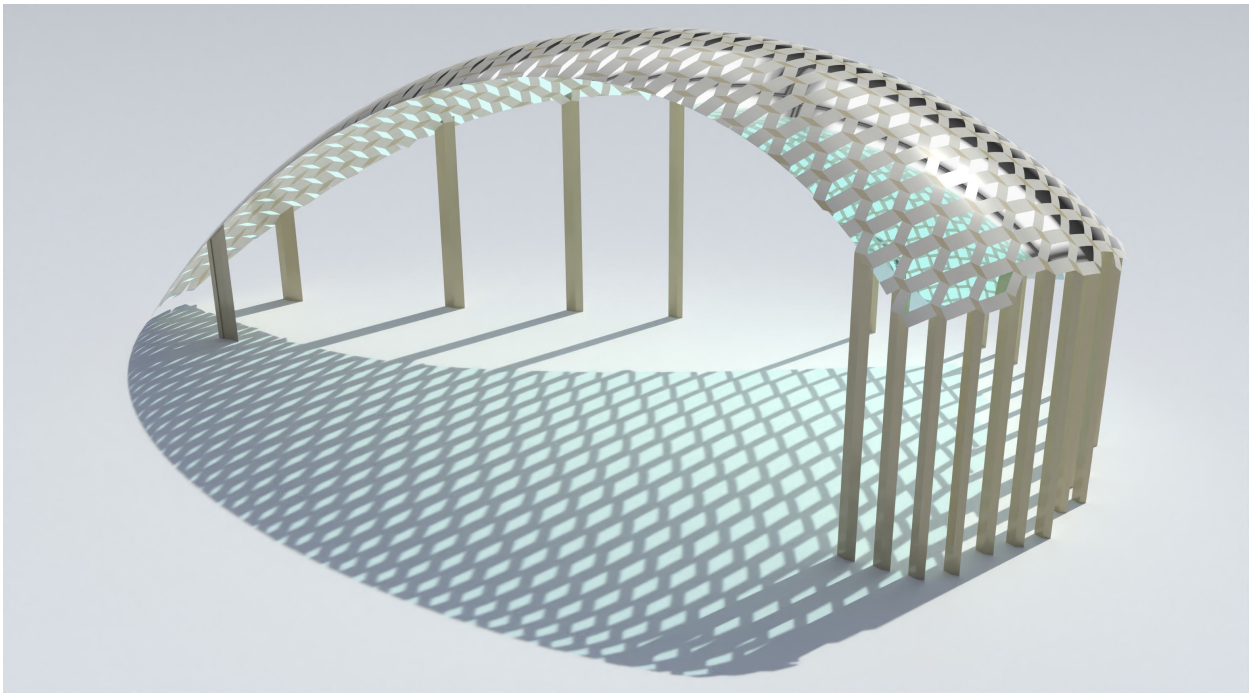

**Figure 2:** Roof concept design based on a portion of an L-net (shown in Fig. 3), illustrating the watertight surface generated from the corresponding L-net structure.

## 1.2. Related work

In view of the recent study of meshes with spherical faces within Möbius geometry (Kilian et al., 2023; Ramos-Cisneros et al., 2024), we keep the overview of prior research short and refer for more details to the extensive literature reviews in these papers.

Our motivation for the research on spherical panel meshes is rooted in the paneling of architectural freeform skins (Eigensatz, Kilian, Schiftner, Mitra, Pottmann and Pauly, 2010; Pottmann et al., 2015), especially in solutions based on quad meshes with planar faces (Q-nets). Since they are discrete counterparts to conjugate parameterizations of surfaces, the major approach for approximating with Q-nets at first determines a conjugate direction field on the given reference surface. Quad remeshing along these directions and post-optimization yield the final approximating Q-net (see e.g. (Liu et al., 2006; Liu, Xu, Wang, Zhu, Guo, Chen and Wang, 2011; Zadravec, Schiftner and Wallner, 2010)). There is a large space of possible conjugate direction fields. A very recent contribution employs a data-driven approach based on neural networks to generate conjugate direction fields guided by user-specified strokes on the surface, avoiding expensive nonlinear optimization (Tao, Yang and Deng, 2025).

In geometry processing, sphere meshes or approximations of surfaces with spherical faces occur, for example, in (Jadon, Thomaszewski, Apolinarska and Poranne, 2022; Thiery, Guy and Boubekeur, 2013; Thiery, Guy, Boubekeur and Eisemann, 2016; Tkach, Pauly and Tagliasacchi, 2016).

Sphere geometries, especially from a differential geometric perspective, are treated in the monographs by Blaschke (1929) and Hertrich-Jeromin (2003); a more recent exposition focusing on non-Euclidean Laguerre geometry is presented in (Bobenko, Lutz, Pottmann and Techter, 2021).

Contributions to discrete differential sphere geometry include work on the Willmore energy for triangle meshes (Bobenko and Schröder, 2005), discrete principal nets (Bobenko and Suris, 2006, 2008, 2007; Liu et al., 2006), their extension to smooth cyclidic nets (Bobenko and Huhnen-Venedey, 2012) and principal symmetric nets (Pellis et al., 2020), as well as more recent discretizations of principal parametrizations such as checkerboard patterns (Peng, Jiang, Wonka and Pottmann, 2019; Dellinger, 2024) and principal binets (Affolter and Techter, 2026), formulated within Lie, Möbius, and Laguerre geometry.

| Basic objects of Laguerre geometry | | Discrete and smooth L-conjugate nets | |
|---|---|---|---|
| **Euclidean model (2.1)** | **Cyclographic model (2.2)** | **Euclidean model (2.3,3.2)** | **Cyclographic model (2.3,3.1)** |
| Oriented sphere | Point in $\mathbb{R}^{3,1}$ | Vertex sphere | Point-vertex in $\mathbb{R}^{3,1}$ |
| Oriented cone | Space-like line | Edge cone | Space-like edge |
| Oriented plane | $\gamma$-hyperplane | Face plane | $\gamma$-hyperplane attached to face |
| Oriented contact w. plane | Incidence w. $\gamma$-hyperplane | Oriented contact cone-plane | Incidence edge–$\gamma$-hyperplane |
| Laguerre transformation | Minkowski similarity | Sphere congruence | Net in $\mathbb{R}^{3,1}$ |
| Offsetting operation | $x_4$-parallel translation | Net in $\mathbb{R}^3$ | $\gamma$-hyperplane congruence |

**Table 1**
The informal correspondence between the Euclidean and the cyclographic model of Laguerre geometry. Note that a net in $\mathbb{R}^{3,1}$ corresponds to a sphere congruence in $\mathbb{R}^3$ and a net in $\mathbb{R}^3$ corresponds to a $\gamma$-hyperplane congruence in $\mathbb{R}^{3,1}$. For details, we refer to section numbers in parentheses.

Applications of Laguerre geometry in CAGD have so far mainly dealt with problems in algebraic geometry, such as rational offset families of curves or surfaces (Peternell and Pottmann, 1998; Pottmann and Peternell, 1998). We will also use the cyclographic model of Laguerre geometry in 4-dimensional Minkowski space. In this context, we refer to remarkable recent contributions on special quad meshes in Minkowski 3-space and their close relation to certain models in statistical mechanics (Affolter, Dellinger, Müller, Polly and Smeenk, 2024, 2025). The isotropic model of Laguerre geometry is yet another classical model with nice applications, e.g., in CNC machining (Pottmann, Grohs and Mitra, 2009; Skopenkov, Bo, Bartoň and Pottmann, 2020; Skopenkov, Pottmann and Grohs, 2012).

## 2. A few basics of Laguerre geometry and L-nets

In this section, we provide a very short outline of Laguerre sphere geometry and quad meshes with square grid combinatorics, called L-nets, in this geometry. We do that in 3-dimensional Euclidean space (informally referred to as *Euclidean model* of Laguerre geometry; Sec. 2.1) and the so-called cyclographic model in 4-dimensional Minkowski space (Sec. 2.2). We connect the models in Tab. 1 serving as a road-map of Secs. 2–3. In the latter model, L-nets are probably more easily understood than in the Euclidean model. Most importantly, the cyclographic model is particularly useful for the discussion of smooth analogs of L-nets and the associated concept of L-conjugacy (see Sec. 3).

For detailed discussions of Laguerre geometry and its various models, we refer to (Blaschke, 1929; Cecil, 2008; Pottmann and Peternell, 1998).

### 2.1. Laguerre Geometry in 3-dimensional Euclidean space

First, we outline the main concepts informally, and then give rigorous definitions. The basic elements of Laguerre sphere geometry in Euclidean space $\mathbb{R}^3$ are *oriented spheres* and *oriented planes*. *Orientation* is understood as the choice of a continuous family of unit normal vectors at all points of a surface. *Oriented contact* between elements means tangency and agreement in orientation. Oriented spheres are allowed to have zero radius, i.e. degenerate to points; in this case, oriented contact is defined separately. Laguerre geometry studies properties of its elements that are invariant under *Laguerre transformations* (see Fig. 5). These are pairs of bijective transformations of the sets of oriented spheres and oriented planes, respectively, preserving oriented contact. For example, an *offsetting transformation* takes an oriented plane or an oriented sphere to its offset at a fixed distance in the direction of the chosen normal. Laguerre transformations do not necessarily preserve points, as those are viewed as spheres of zero radius and can be mapped to other spheres. Likewise, lines can be mapped to *oriented cones*. We may view an oriented cone as the envelope of oriented tangent planes that are in oriented contact with two distinct oriented spheres. Oriented cones may degenerate to cylinders or lines and are preserved under Laguerre transformations.

Let us discuss these notions systematically and provide precise definitions.

*Oriented spheres* An *oriented sphere*, shortly *or-sphere*, is either a Euclidean sphere in $\mathbb{R}^3$ equipped with a continuous family of unit normal vectors at all points, or a point in $\mathbb{R}^3$. An or-sphere is given by its center $c \in \mathbb{R}^3$ and *signed radius* $r \in \mathbb{R}$, which is defined as follows. If the normals point inward, i.e., toward its center, the *signed radius* is the radius (with a positive sign). For outward-pointing normals, the *signed radius* is minus the radius (i.e., the radius with a negative sign). For a point, the *signed radius* is zero.

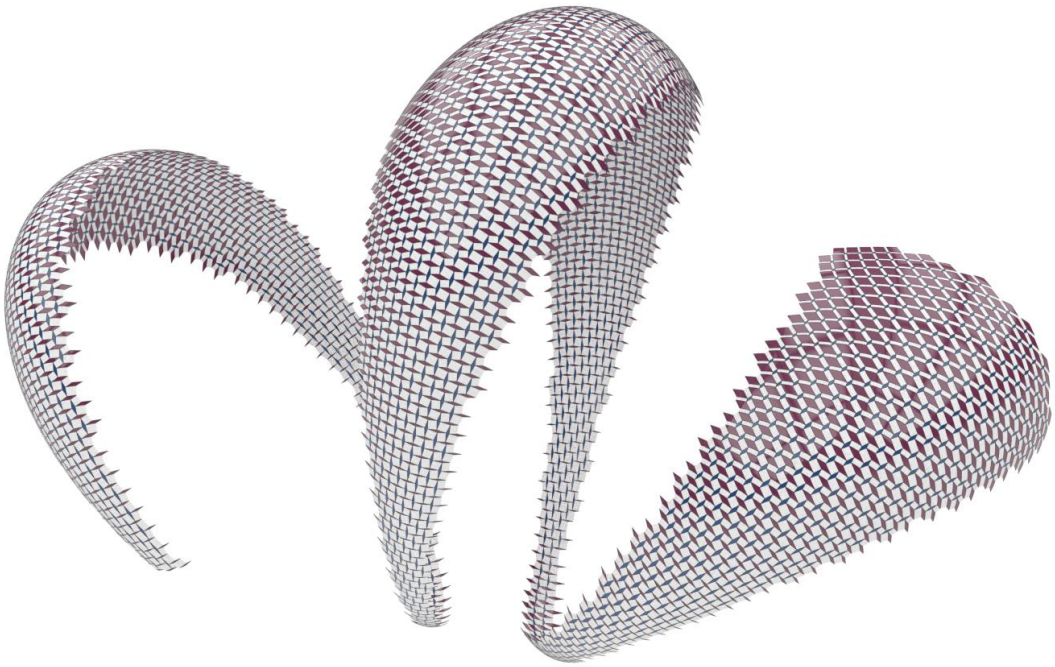

**Figure 3:** L-net approximation of a spiral-like surface. Smaller spherical panels appear in the narrow regions of the surface, whereas larger spherical panels arise in the wider regions.

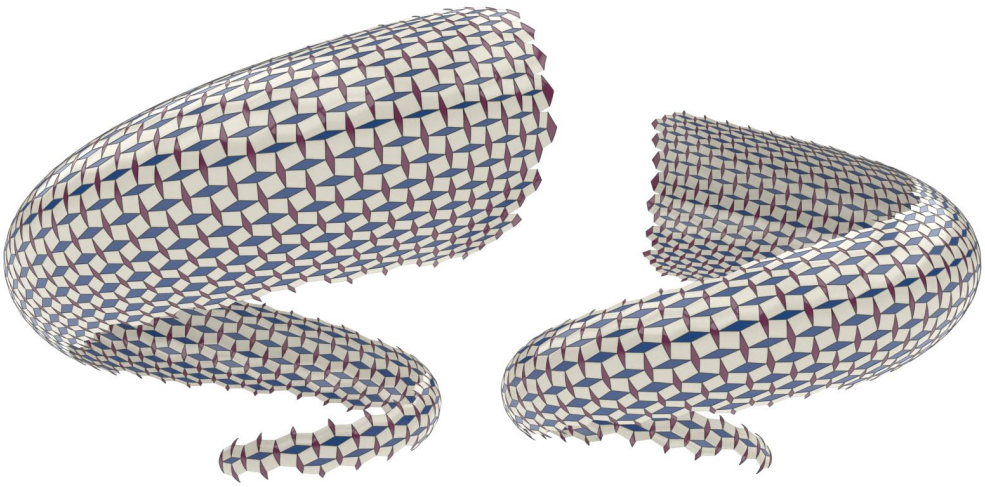

**Figure 4:** L-net approximation of a seashell-like surface.

*Oriented planes* An *oriented plane* (*or-plane*) $p$ is a plane in $\mathbb{R}^3$ equipped with a continuous family of unit normal vectors at all points (which is therefore the same vector $n$ at all points). An or-plane $p$ is given by its unit normal vector $n$ and the *signed distance* $h$ to the origin, which is defined as follows. If the plane contains the origin, the *signed distance* is zero. Otherwise, if the normal $n$ points toward the origin, the *signed distance* is the distance (with a positive sign). If the normal points in the opposite direction, the *signed distance* is minus the distance.

The plane $p$ is thus the set of all $x \in \mathbb{R}^3$ satisfying the equation

$$\langle n, x \rangle + h = 0. \tag{1}$$

*Oriented contact* *Oriented contact* (*or-contact*) of oriented spheres/planes means tangency in the usual sense and agreement of unit normals at a contact point. A point is in *oriented contact* with an oriented sphere/plane if it lies on the sphere/plane. Thus, the or-plane $p$ is in oriented contact with an oriented sphere $s = (c, r)$ with center $c \in \mathbb{R}^3$ and signed radius $r$ if and only if $p$ has *signed distance* $r$ from $c$, i.e.

$$\langle n, c\rangle + h = r. \tag{2}$$

*Laguerre transformations* *Laguerre transformations* are pairs of bijective transformations of the sets of or-spheres and or-planes, respectively, preserving oriented contact. A simple example is the *$d$-offsetting operation* which adds the same constant $d$ to the signed radius $r$ of each or-sphere and to the signed distance $h$ from each or-plane to the origin, while preserving the centers $c$ of or-spheres and the normal vectors $n$ of or-planes. By (2), this transformation preserves the or-contact between or-spheres and or-planes. Euclidean isometries of $\mathbb{R}^3$ are also Laguerre transformations.

*Oriented cones* A *rotational cone* is the union of lines (*rulings*) passing through a fixed point (*vertex*) and forming a fixed angle (nonzero and non-right) with a fixed line in $\mathbb{R}^3$ passing through the fixed point. An *oriented rotational cone* is a rotational cone equipped with a continuous family of unit normal vectors at all points (excluding the vertex) such that the normal vectors along each ruling are the same. (The latter requirement is needed because the cone without the vertex splits into two components, which a priori can be oriented independently.) An *oriented rotational cylinder* is the union of lines at a fixed nonzero distance from a fixed line, equipped with a continuous family of unit normal vectors at all points. A *generalized oriented cone* (*or-cone*) is an oriented rotational cone or oriented rotational cylinder or (non-oriented) straight line in $\mathbb{R}^3$.

*Oriented contact* between an or-plane and a two-dimensional or-cone means tangency in the usual sense and agreement of unit normals at a contact point (distinct from the cone vertex). *Oriented contact* between an or-plane and a line means that the line is contained in the or-plane.

The set of or-planes in oriented contact with an or-cone coincides with the set of or-planes in oriented contact with a fixed pair of spheres $s_i = (c_i, r_i)$, where $i = 0, 1$. Namely, for an oriented rotational cone, these two spheres have radii $r_0 \neq r_1$, for an oriented rotational cylinder, we have $r_0 = r_1 \neq 0$, and for a straight line, we have $r_0 = r_1 = 0$. The or-spheres $s_0$ and $s_1$ must have common oriented tangent planes, which requires $\|c_0 - c_1\|^2 > (r_0 - r_1)^2$.

All the or-spheres in the *linear family* $s(t) := (1-t)s_0 + ts_1 := \big((1-t)c_0 + tc_1, (1-t)r_0 + tr_1\big)$, where $t \in \mathbb{R}$, are also in oriented contact with all those or-planes. Any of the or-spheres $s(t)$ is referred to as an or-sphere *in oriented contact with the or-cone along a circle*. In particular, a point $s(t)$ (the or-sphere with $r(t) := (1-t)r_0 + tr_1 = 0$) is the vertex of the cone or a point of the straight line to which the or-cone degenerates in case of $r_0 = r_1 = 0$; it is still viewed as having *oriented contact with the or-cone along a circle*.

We use $\mathrm{OrSpheres}(\mathbb{R}^3)$ to denote the set of or-spheres, $\mathrm{OrPlanes}(\mathbb{R}^3)$ for the set of or-planes, and $\mathrm{OrCones}(\mathbb{R}^3)$ for the set of or-cones.

## 2.2. Cyclographic Model

The cyclographic model of Laguerre geometry considers an oriented sphere $s = (c, r)$ with center $c = (c_1, c_2, c_3) \in \mathbb{R}^3$ and signed radius $r$ as a point $S = (c_1, c_2, c_3, r)$ in Minkowski space $\mathbb{R}^{3,1}$ with the inner product $\langle\!\langle \cdot, \cdot \rangle\!\rangle$ of signature $(+,+,+,-)$. The map $\zeta : s \mapsto S$ is called the *Minkowski lift*, and its inverse $\zeta^{-1}$ is the *cyclographic map*; see Tab. 1.

The Minkowski lift of the or-plane $p$ is defined as the set of points $X = (x, x_4) \in \mathbb{R}^{3,1}$, taken to or-spheres in oriented contact with $p$ by the cyclographic map. By (1) and (2), this is expressed as

$$x_4 = \langle n, x\rangle + h, \tag{3}$$

and represents a hyperplane $P =: \zeta(p) \subset \mathbb{R}^{3,1}$ forming the Euclidean angle $\gamma = \pi/4$ with the hyperplane $\mathbb{R}^3$ given by $x_4 = 0$. A hyperplane of form (3) is called a *$\gamma$-hyperplane* or *isotropic hyperplane*. We denote by $\Gamma(\mathbb{R}^{3,1})$ the set of all $\gamma$-hyperplanes. Note that (3) can be written with the isotropic normal vector $N = (n, 1)$ that is both normal and parallel to the hyperplane, as

$$\langle\!\langle N, X \rangle\!\rangle + h = 0.$$

*Lines in Minkowski space* A line in Minkowski space is called *space-like*, *light-like* (*isotropic*), or *time-like*, respectively, if its direction vector $g$ satisfies $\langle\!\langle g, g \rangle\!\rangle > 0$, $\langle\!\langle g, g \rangle\!\rangle = 0$, $\langle\!\langle g, g \rangle\!\rangle < 0$, respectively. The cyclographic image of a space-like line is a family of or-spheres in oriented contact with an or-cone along a circle, and the line

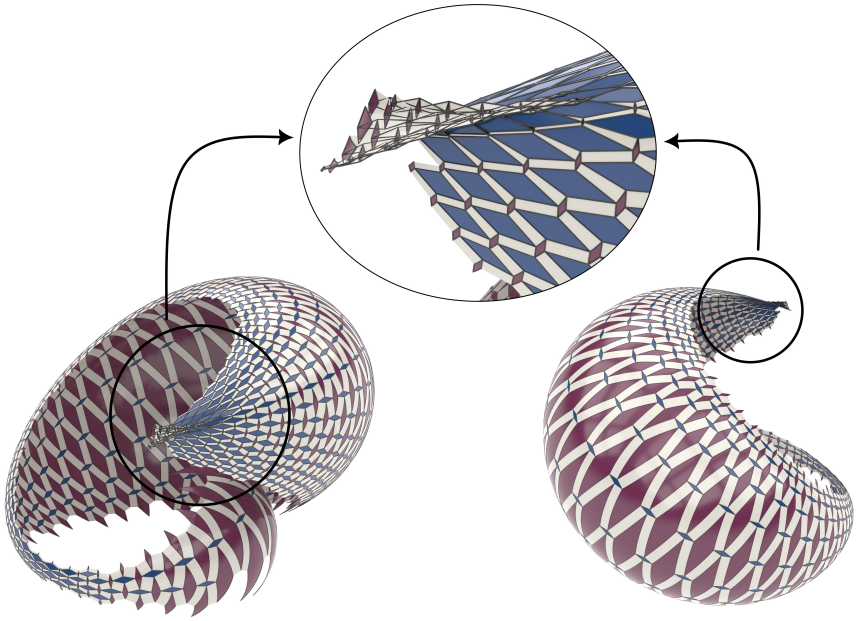

**Figure 5:** A Laguerre transformation of the L-net in Fig. 4. While such transformations offer a tool for exploring different designs, singularities may emerge in the process. The inset shows a close-up of a region where singularities appear.

is viewed as the *Minkowski lift* of that or-cone. The cyclographic image of an isotropic line is a family of or-spheres tangent to each other at a single point and sharing the same tangent plane there (thus forming a *contact element*, but we do not need this terminology). A time-like line corresponds to a family of or-spheres whose centers lie on a fixed line orthogonal to a plane, while all spheres intersect that plane at a constant angle.

*Planes in Minkowski space* A 2-dimensional plane in $\mathbb{R}^{3,1}$ is called *space-like*, *light-like (isotropic)*, or *time-like* if it contains zero, one, or two isotropic lines through each point, respectively.

*Laguerre transformations* In $\mathbb{R}^{3,1}$, Laguerre transformations appear as those bijective affine maps which map isotropic lines to isotropic lines. This implies that isotropic planes, characterized by containing a single real family of parallel isotropic lines, are mapped to isotropic planes. Hence, in $\mathbb{R}^3$, we have two bijective maps of the sets of or-spheres and or-planes, respectively, which preserve oriented contact (Fig. 5). These transformations correspond to Minkowski similarities of $\mathbb{R}^{3,1}$, generated by the orthogonal group $O(3,1)$, translations, and scalings. For instance, the $d$-offsetting operation appears as the translation $x_4 \mapsto x_4 + d$ in $\mathbb{R}^{3,1}$.

## 2.3. L-nets

We are now ready to define the main objects of interest, namely quad meshes with square grid combinatorics in Laguerre geometry. We call them L-nets and define them as follows (see Fig. 6 to the left).

**Definition 2.1** (L-net)**.** *An $m \times n$ **square grid** is the plane graph with the vertices at integer points $(i, j)$, where $0 \le i \le n$, $0 \le j \le m$, and edges joining the vertices at unit distance. Denote by $V$ the set of vertices, by $E$ the set of edges, and by $F$ the set of bounded faces of the square grid. An **L-net** in $\mathbb{R}^3$ is a triple of maps*

$$\mathcal{V}_{\mathcal{S}} : V \to \mathrm{OrSpheres}(\mathbb{R}^3), \quad \mathcal{E}_{\mathcal{C}} : E \to \mathrm{OrCones}(\mathbb{R}^3), \quad \mathcal{F}_{\mathcal{P}} : F \to \mathrm{OrPlanes}(\mathbb{R}^3),$$

*satisfying the following conditions:*

- *if an edge $e \in E$ contains a vertex $v \in V$, then the or-cone $\mathcal{E}_{\mathcal{C}}(e)$ is in oriented contact with the or-sphere $\mathcal{V}_{\mathcal{S}}(v)$ along a circle;*
- *if an edge $e \in E$ meets a face $f \in F$, then the or-cone $\mathcal{E}_{\mathcal{C}}(e)$ is in oriented contact with the or-plane $\mathcal{F}_{\mathcal{P}}(f)$ along a ruling.*

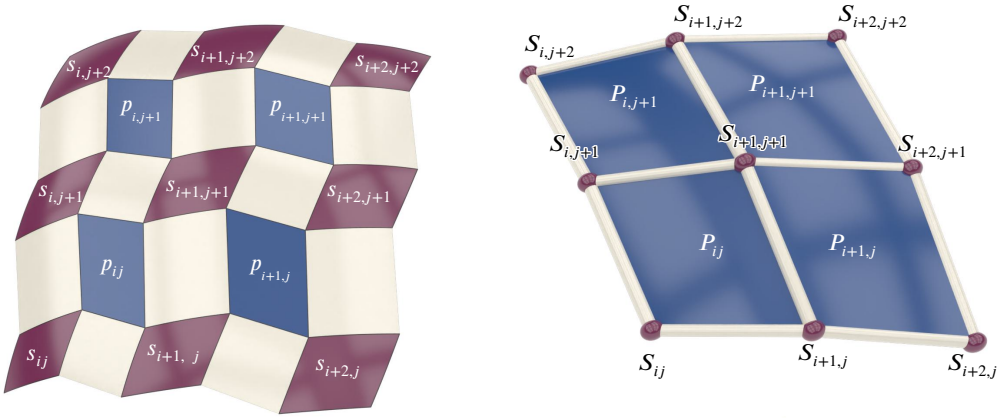


**Figure 6:** L-net elements. (Left) Euclidean model of Laguerre geometry; (right) cyclographic model.

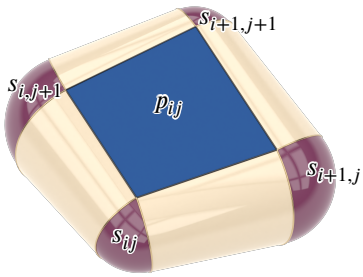


Our notation indicates that we view the or-spheres as vertices, the or-planes as faces , and the or-cones as edges. Quadrilateral patches of or-planes, or-cones, and or-spheres of an L-net define a surface $\mathcal{L}$ as shown in the inset and Fig. 1. We assume that the figure is self-explanatory and do not further detail the boundaries of these patches. We see that $\mathcal{L}$ can be a $C^1$ surface.

The definition extends to more general combinatorics, because the oriented contact conditions are imposed locally. For simplicity, we restrict our study to square grid combinatorics; the general case is the subject of ongoing work.

For each vertex $(i, j) \in V$, denote $s_{ij} := \mathcal{V}_{\mathcal{S}}(i, j)$. For a face $f$ with the vertices $(i, j)$, $(i + 1, j)$, $(i + 1, j + 1)$, $(i, j + 1)$ (see inset figure), denote $p_{ij} := \mathcal{F}_{\mathcal{P}}(f)$. Sometimes, we also denote by $\mathcal{V}_{\mathcal{S}}$ and $\mathcal{F}_{\mathcal{P}}$ the images of the maps $\mathcal{V}_{\mathcal{S}}$ and $\mathcal{F}_{\mathcal{P}}$.

*Examples of L-nets* If all spheres $s_{ij}$ of an L-net are points, we get a Q-net (quad mesh with planar faces). Q-nets are discrete conjugate surface parameterizations and have played a fundamental role in the development of discrete differential geometry (Bobenko and Suris, 2008). To obtain a less degenerate appearance of the L-net, we may apply a Laguerre transformation, for example, a $d$-offsetting operation. Now all spheres have radius $d$ and edge cones are cylinders of radius $d$. That L-net represents a smooth surface in "positively curved" areas, but has singularities in areas of "negative curvature"; see Fig. 7.

A special case of the previous example is an L-net in which the four or-planes in or-contact with an or-sphere $s_{ij}$ are in or-contact with another or-sphere $\bar{s}_{ij}$, and thus are in or-contact with an or-cone $c_{ij}$ that is in or-contact with $s_{ij}$ and $\bar{s}_{ij}$ along circles. If spheres $s_{ij}$ are points, such an L-net is a *conical net*, known as a Laguerre geometric object and a discrete principal curvature parameterization (Bobenko and Suris, 2008; Liu et al., 2006). It gives rise to infinitely many less degenerate L-nets, since we can replace the point $s_{ij}$ with any sufficiently small or-sphere $s'_{ij}$ in oriented contact with $c_{ij}$ along a circle, while keeping all the or-planes $p_{ij}$ and adjusting the edges of the L-net accordingly. The freedom in choosing the sphere radius provides a simple solution to our approximation problem. We may approximate the given surface $f$ by a conical net, obtained by computing principal curvature directions on $f$, extracting a quad mesh aligned with these directions, and optimizing it to satisfy the conical net constraints (Liu et al., 2006), and then modify it to an L-net by replacing the vertices with spheres that are close to the prescribed spheres $s_f$ tangent to $f$.

This solution is very restricted. We will see that there is a much larger variety of solutions that may be preferred in a given application.

*L-nets in the cyclographic model* In the cyclographic model, an L-net is a quad mesh with square grid combinatorics in $\mathbb{R}^{3,1}$ (see Fig. 6 to the right). Its vertices $S_{ij}$ are the Minkowski lifts of the or-spheres $s_{ij}$. Its edges are segments of space-like lines and represent the edge cones. Its faces $P_{ij}$ are not necessarily planar quadrilaterals

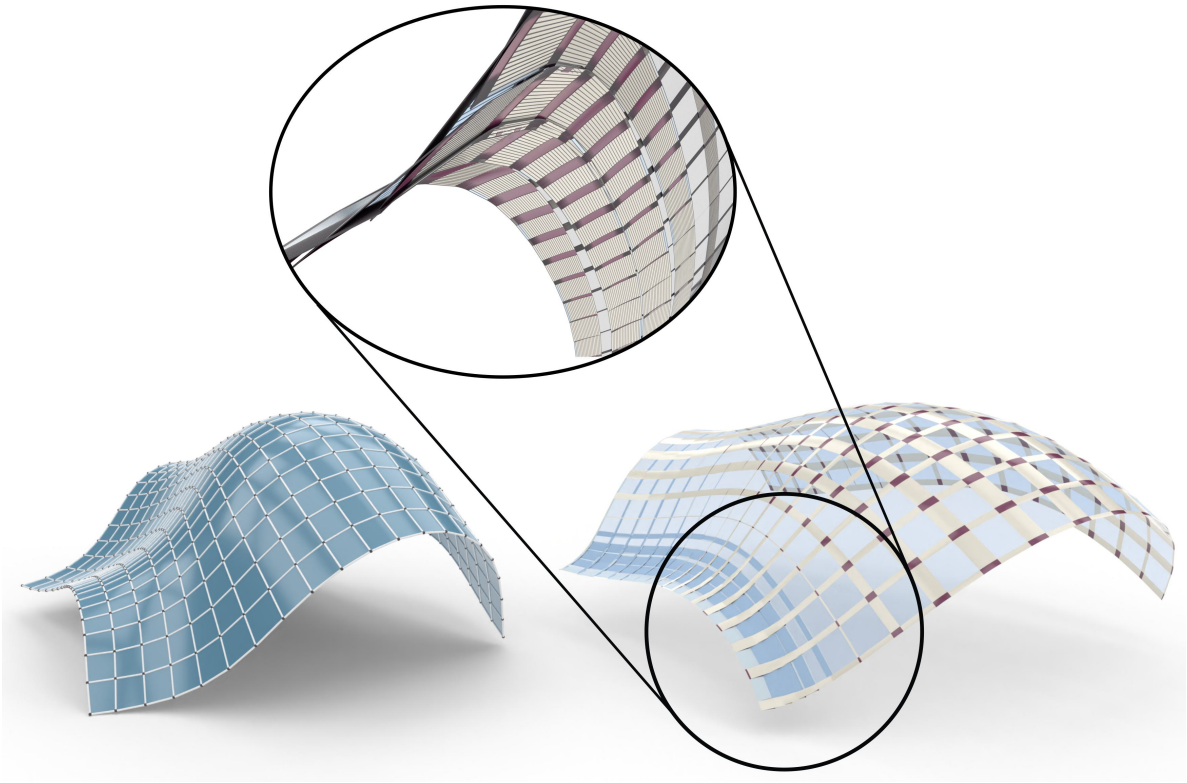

**Figure 7:** A Q-net (left) extended to an L-net (right) by offsetting. Spheres are shown in red and planar faces as translucent blue panels to reveal the singular behavior. The inset highlights the bottom view of the swallowtail singularities arising in regions of "negative curvature".

$S_{i-1,j-1}S_{i,j-1}S_{ij}S_{i-1,j}$, lying in the isotropic hyperplanes corresponding to the planes $p_{ij}$. This leads to the following definition; the Minkowski lift then induces a one-to-one correspondence between L-nets in $\mathbb{R}^3$ and $\mathbb{R}^{3,1}$.

**Definition 2.2** (L-net)**.** *Let* $\mathrm{Graff}_1^+(\mathbb{R}^{3,1})$ *be the set of space-like lines in* $\mathbb{R}^{3,1}$*. An* ***L-net*** *in* $\mathbb{R}^{3,1}$ *is a triple of maps*

$$S : V \to \mathbb{R}^{3,1}, \;\; C : E \to \mathrm{Graff}_1^+(\mathbb{R}^{3,1}), \;\; P : F \to \Gamma(\mathbb{R}^{3,1}),$$

*preserving incidences, i.e., for any* $v \in V$*,* $e \in E$*, and* $f \in F$*, the inclusion* $v \subset e$ *implies* $S(v) \subset C(e)$ *and* $e \subset f$ *implies* $C(e) \subset P(f)$*.*

*L-net as discrete surface and attached sphere congruence* We conclude this section by sketching the informal meaning of the notion of an L-net. Namely, an L-net can be viewed as a discrete version of a 2-dimensional set of or-planes that may be seen as oriented tangent planes of a surface $f(u, v)$ in $\mathbb{R}^3$. Moreover, it is also a discrete version of a 2-dimensional set of or-spheres $s(u, v)$ that are tangent to the surface $f$. Such a set of spheres is often called a sphere congruence. Hence, we have a discrete dual (i.e., plane based) representation of a surface $f$ and a sphere congruence $s$ that is tangent to $f$, in other words, sphere congruence $s$ attached to the surface $f$. It is important to note that an L-net is therefore not a discretization of a general sphere congruence or of a general tangent plane congruence, but rather the special case in which the two are coupled through this oriented contact, as developed in the following sections.

Moving to the cyclographic model, we have a discrete 2-dimensional surface $S$ and an attached set of isotropic hyperplanes. Note that the role of the surface and the attached sphere/hyperplane congruence has now been swapped. These hyperplanes define one "discrete envelope" of the discrete sphere congruence. The other "discrete envelope" is in general not represented as an L-net. The smooth counterpart is a surface $S(u, v)$ and an attached set of tangent isotropic hyperplanes $P(u, v)$ that define one envelope of the sphere congruence $s(u, v)$ in $\mathbb{R}^3$. This smooth analog will be discussed in the next two sections in detail, as it provides the key for the approximation of a given surface $f$ by an L-net whose or-spheres are close to a given sphere congruence $s(u, v)$ attached to $f$.

## 3. Smooth L-nets and L-conjugacy

We are now ready to present the main concept of our paper, namely, smooth L-nets. They are L-conjugate nets on a surface with respect to an attached sphere congruence. Since the appearance of L-nets in the cyclographic model is simpler and quite close to the familiar Q-nets, we prefer to start our study there (Section 3.1) and then turn to the Euclidean model of Laguerre geometry in Section 3.2.

### 3.1. L-conjugacy in the cyclographic model

Recall that an L-net in $\mathbb{R}^{3,1}$ is a quad mesh $S$ whose faces lie in isotropic hyperplanes $P_{ij}$. The smooth analog is a surface $S(u,v)$ with an attached family of tangent isotropic hyperplanes $P(u,v)$. As analogs of faces in $S$, hyperplanes $P(u,v)$ contain the partial derivatives $S_u, S_v, S_{uv}$. The situation is similar to Q-nets and their smooth analogs, where conjugacy requires $S_{uv}$ to lie in the tangent plane spanned by $S_u, S_v$; analogously, L-conjugacy requires $S_{uv}$ to lie in the attached isotropic hyperplane $P(u,v)$. This motivates the following definition. Recall that $\Gamma(\mathbb{R}^{3,1})$ is the set of all isotropic hyperplanes in $\mathbb{R}^{3,1}$.

**Definition 3.1** (L-conjugate net)**.** *Throughout, $S:\mathbb{R}^2\to\mathbb{R}^{3,1}$ is a **regular smooth space-like or light-like net**, that is, a smooth map such that $S_u(u,v)$ and $S_v(u,v)$ span a 2-dimensional space-like or light-like plane at each point $(u,v)\in\mathbb{R}^2$. We equip it with an **attached tangent isotropic hyperplane congruence** $P:\mathbb{R}^2\to\Gamma(\mathbb{R}^{3,1})$, that is, a smooth map such that the hyperplane $P(u,v)\ni S(u,v)$ and $P(u,v)\parallel S_u(u,v), S_v(u,v)$ at each point $(u,v)\in\mathbb{R}^2$.*

*The net $S$ is called an **L-conjugate net** in $\mathbb{R}^{3,1}$ with respect to the attached congruence $P$ if $S_u, S_v, S_{uv}$ are parallel to $P(u,v)$ at each point $(u,v)\in\mathbb{R}^2$.*

**Remark 3.2.** *Generically, the isotropic hyperplane $P(u,v)$ is uniquely determined by $S_u, S_v, S_{uv}$, except for the special case where $S_u, S_v, S_{uv}$ are linearly dependent and their span reduces to the tangent plane at $S(u,v)$, when it is precisely a conjugate net in the usual sense. In the case where the tangent plane is space-like, there are exactly two isotropic hyperplanes through it. As we shall see in a subsequent publication, then both envelopes of the sphere congruence in the Euclidean model of Laguerre geometry are represented by L-conjugate nets.*

The net $S$ takes a sufficiently small neighborhood of each point $(u,v)\in\mathbb{R}^2$ to a smooth surface in $\mathbb{R}^{3,1}$, still denoted by $S$ (by a slight abuse of notation). For our application, it is important to define L-conjugate tangent directions of the surface $S$ and not just an entire L-conjugate parameterization. Moreover, we need to be able to compute L-conjugate directions from any parameterization of $S$. We therefore arrive at the following "self-evident" definition.

**Definition 3.3** (L-conjugate tangents)**.** *A **reparametrization** of the pair $(S,P)$ is a pair of maps $(S\circ D, P\circ D)$ for some diffeomorphism $D:\mathbb{R}^2\to\mathbb{R}^2$. Two tangents $T_1\neq T_2$ (or tangent vectors $T_1 \nparallel T_2$) at a surface point $X=S(u,v)\in\mathbb{R}^{3,1}$ are called **L-conjugate** with respect to the attached congruence $P$ if there is a reparametrization $(\bar S,\bar P)$ of $(S,P)$ such that $\bar S_u\parallel T_1$, $\bar S_v\parallel T_2$, and $\bar S_u, \bar S_v, \bar S_{uv}\parallel\bar P$ at the point $X$.*

The remainder of this subsection aims to find a simple characterization of L-conjugate tangents in terms of an arbitrary parameterization $S$.

First, we obtain a characterization in terms of an analog of the second fundamental form.

**Theorem 3.4.** *Two non-parallel tangent vectors $A=a_1S_u+a_2S_v$ and $B=b_1S_u+b_2S_v$ at a surface point $S(u,v)\in\mathbb{R}^{3,1}$ are L-conjugate with respect to the attached congruence $P$ if and only if*

$$\mathrm{II}_{S,P,N}(A,B) := L_{S,P,N}a_1b_1 + M_{S,P,N}(a_1b_2+a_2b_1) + N_{S,P,N}a_2b_2 = 0, \tag{4}$$

*where*

$$\begin{aligned} L_{S,P,N} &:= \langle\!\langle S_{uu}, N\rangle\!\rangle = -\langle\!\langle S_u, N_u\rangle\!\rangle,\\ M_{S,P,N} &:= \langle\!\langle S_{uv}, N\rangle\!\rangle = -\langle\!\langle S_u, N_v\rangle\!\rangle = -\langle\!\langle S_v, N_u\rangle\!\rangle,\\ N_{S,P,N} &:= \langle\!\langle S_{vv}, N\rangle\!\rangle = -\langle\!\langle S_v, N_v\rangle\!\rangle, \end{aligned} \tag{5}$$

*and $N(u,v)$ is a normal vector to $P(u,v)$ smoothly depending on $(u,v)$.*

*Proof.* By the definition of an attached tangent isotropic hyperplane congruence $P$ and a normal vector $N$, we have

$$\langle\langle S_u, N\rangle\rangle = \langle\langle S_v, N\rangle\rangle = 0. \tag{6}$$

Differentiating the latter equation, we get $\langle\langle S_{uu}, N\rangle\rangle = -\langle\langle S_u, N_u\rangle\rangle$ and the other equalities in (5). Thus

$$\begin{aligned}\mathrm{II}_{S,P,N}(A,B) &= -\langle\langle S_u, N_u\rangle\rangle a_1 b_1 - \langle\langle S_u, N_v\rangle\rangle a_1 b_2 - \langle\langle S_v, N_u\rangle\rangle a_2 b_1 - \langle\langle S_v, N_v\rangle\rangle a_2 b_2 \\ &= -\langle\langle a_1 S_u + a_2 S_v, b_1 N_u + b_2 N_v\rangle\rangle = -\langle\langle A, \frac{\partial N}{\partial B}\rangle\rangle. \end{aligned} \tag{7}$$

(In the latter expression, by a slight abuse of notation, $N$ is viewed as a function in a vicinity of the point $S(u,v)$ on $S(\mathbb{R}^2)$ and $\frac{\partial N}{\partial B}$ is its derivative in the $B$-direction.) Since $\frac{\partial N}{\partial B}$ is invariant under reparametrizations, $\mathrm{II}_{S,P,N}(A,B)$ is, that is, $\mathrm{II}_{S,P,N}(A,B) = \mathrm{II}_{\bar{S},\bar{P},N}(A,B)$ for any reparametrization $(\bar{S},\bar{P})$. In particular, if $\bar{S}_u = A$ and $\bar{S}_v = B$, we get

$$\mathrm{II}_{\bar{S},\bar{P},N}(A,B) = M_{\bar{S},\bar{P},N} = \langle\langle \bar{S}_{uv}, N\rangle\rangle.$$

Now, if $A$ and $B$ are L-conjugate with respect to $P$, then $\bar{S}_{uv} \parallel \bar{P}$ for suitable reparametrization, hence $\mathrm{II}_{S,P,N}(A,B) = \mathrm{II}_{\bar{S},\bar{P},N}(A,B) = 0$. Conversely, if $\mathrm{II}_{S,P,N}(A,B) = 0$, then for any reparametrization $(\bar{S},\bar{P})$ such that $\bar{S}_u \parallel A$ and $\bar{S}_v \parallel B$, we have $\bar{S}_{uv} \parallel \bar{P}$ (in particular, such a reparametrization exists), hence $A$ and $B$ are L-conjugate with respect to $P$. □

Note that $\mathrm{II}_{S,P,N}(A,B)$ depends on the choice of the normal vector $N$, but the condition $\mathrm{II}_{S,P,N}(A,B) = 0$ is invariant. This theorem suggests the following extension of our definition.

**Definition 3.5** (Self-L-conjugate tangents)**.** *A tangent $T$ with a direction vector $A$ is **L-conjugate** to itself with respect to $P$ if $\mathrm{II}_{S,P,N}(A,A) = 0$ for some (hence any) choice of normal vector $N(u,v)$ to $P(u,v)$.*

Our next result is guided by the following well-known construction of conjugate surface tangents in $\mathbb{R}^3$: Given a curve $c$ on a generic surface $s$, the envelope of tangent planes of $s$ along $c$ is a developable surface, whose rulings are conjugate to the tangents of $c$. This can be seen, for instance, by considering the limit of a strip in a Q-net.

We proceed in a very similar way and first look at the discrete L-net $S$ informally. Polylines $i = \text{const}$ and $j = \text{const}$ are called discrete *parameter lines*. Moreover, we consider *strips*, namely parts of $S$ bounded by adjacent parameter lines, say $i = i_0$ and $i = i_0 + 1$; likewise, we have strips in the other parameter direction. The edges in which adjacent faces of a strip join are called its *transversal edges*. They are discrete tangents and lie in the intersection planes of the isotropic hyperplanes through adjacent faces. These intersection planes are discrete characteristic planes of the discrete envelope of hyperplanes represented by the strip. The discrete view suggests the following concepts.

**Definition 3.6.** *family of hyperplanes $P\colon [0;1] \to \Gamma(\mathbb{R}^{3,1})$ be given by $P(t) : \langle\langle X - S(t), N(t)\rangle\rangle = 0$ for some smooth $S, N : [0;1] \to \mathbb{R}^{3,1}$. The family $P$ is **regular** if $\dot{N} \nparallel N$ for each $t \in [0;1]$. In this case, the union of planes $\Pi(t) := P(t) \cap \dot{P}(t)$ over $t \in [0;1]$, where*

$$\dot{P}(t) : \langle\langle X - S, \dot{N}\rangle\rangle - \langle\langle \dot{S}, N\rangle\rangle = 0,$$

*is called the **envelope of the family** $P$, and each individual plane $\Pi(t)$ is called a **characteristic plane** of the envelope.*

**Proposition 3.7.** *Assume that for a regular smooth curve $C : [0;1] \to S(\mathbb{R}^2)$, $t \mapsto C(t) = S(u(t), v(t))$, the family of hyperplanes $P(u(t), v(t))$ is regular and thus has an envelope $D$. Then, at each point $C(t)$ of $C$, any tangent line to $S(\mathbb{R}^2)$ contained in the characteristic plane $\Pi(t)$ of $D$ is L-conjugate to the tangent of $C$ with respect to $P$.*

*Proof.* The characteristic planes of the envelope $D$ are the planes $P \cap \dot{P}$. If a tangent line is contained in such a plane, the direction vector $\lambda S_u + \mu S_v$ is orthogonal to $\dot{N} = \dot{u} N_u + \dot{v} N_v$, leading to

$$\lambda\dot{u}\langle\langle S_u, N_u\rangle\rangle + \lambda\dot{v}\langle\langle S_u, N_v\rangle\rangle + \mu\dot{u}\langle\langle S_v, N_u\rangle\rangle + \mu\dot{v}\langle\langle S_v, N_v\rangle\rangle = 0.$$

By Theorem 3.4, the vector is L-conjugate to $\dot{C} = \dot{u} S_u + \dot{v} S_v$ with respect to $P$.

□

**Remark 3.8.** *The above results and their proofs remain true without the assumptions that hyperplanes $P$ and therefore normals $N$ are isotropic and the net is space-like or light-like. Hence, here we have a more general concept of conjugacy with respect to an attached set of tangent hyperplanes $P$. Moreover, L-conjugacy is clearly a concept of projective geometry, as is true for ordinary conjugacy in surface theory. We plan to return to this generalization in future work.*

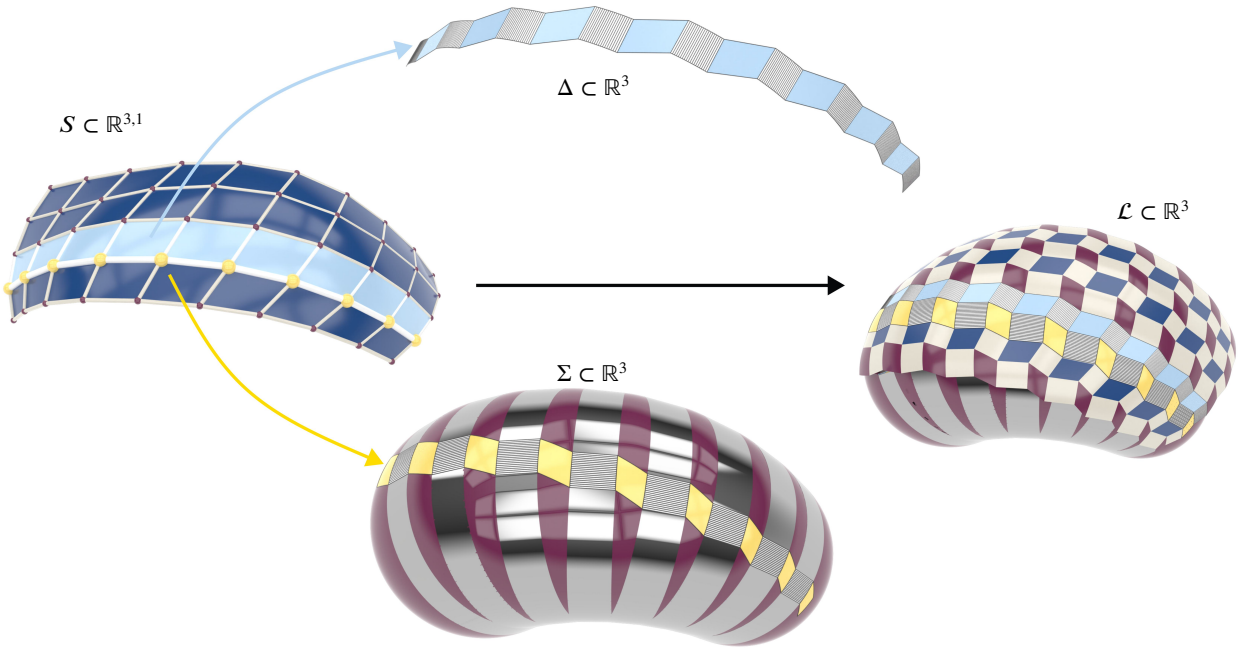


**Figure 8:** A guad mesh $S$ in $\mathbb{R}^{3,1}$ and its corresponding L-net $\mathcal{L}$ in $\mathbb{R}^3$. A parameter line of $S$ (yellow vertices) defines a tangent discrete channel surface $\Sigma$ formed by spheres of the attached congruence joined by or-cones, and a strip of $S$ (light-blue quads) defines a tangent discrete developable surface $\Delta$.

### 3.2. L-conjugacy in Euclidean 3-space

Although it would be possible to base our approximation algorithm on the cyclographic model, it is preferred to work directly in the design space $\mathbb{R}^3$. Thus, we now transfer the results to Euclidean 3-space. This is particularly important for a better understanding of L-conjugacy and its relation to an extended version of curvature theory of surfaces with respect to an attached sphere congruence (see Section 4). We start with an informal motivation, and then give precise definitions.

L-conjugacy in $\mathbb{R}^{3,1}$ has been motivated by geometrically interpreting the edges of the quad mesh $S$ in two ways: as discrete tangents of parameter lines and as tangential components of discrete characteristic planes of envelopes of isotropic hyperplanes.

In $\mathbb{R}^3$, edges of $S$ correspond to or-cones. A discrete parameter line of $S$ corresponds to a discrete set of or-spheres joined by or-cones (Fig. 8). This is a discrete version of a channel surface that is in oriented contact with an oriented surface $f$ and enveloped by spheres taken from the selected attached sphere congruence. In the smooth limit, the rulings of the or-cones correspond to rulings of tangential cones of the channel surface. They are principal curvature directions orthogonal to the characteristic circles.

Strips of $S$ represent strips of an L-net $\mathcal{L}$ which are formed by segments of or-planes and or-cones (Fig. 8). They are discrete models of tangent developable surfaces of a surface $f$, and the rulings of the cones are discrete rulings. The boundaries of the discrete developable strips exhibit, in general, a staircase behavior. However, the discrete rulings change continuously along the strip. We look at the discrete rulings of the strips, which are also cone rulings, to define L-conjugate directions of a surface $f$ with respect to an attached sphere congruence. We shall see that the opposite edges in each vertex quadrilateral should be viewed as two discrete versions of the same direction, and adjacent edges should be viewed as L-conjugate directions. See Fig. 9.

Turning to the smooth setting, we define L-conjugate directions in $\mathbb{R}^3$ therefore as follows.

**Definition 3.9** (L-conjugate net)**.** *Throughout, $f : \mathbb{R}^2 \to \mathbb{R}^3$ is a regular smooth net (a smooth map such that $f_u(u,v) \nparallel f_v(u,v)$ for each $(u,v) \in \mathbb{R}^2$) without parabolic and umbilic points (so that the principal curvatures $\kappa_1$ and $\kappa_2$ are distinct and non-vanishing at each point $(u,v) \in \mathbb{R}^2$). We equip the net with an* ***orientation****, that is, a choice of unit normal $n : \mathbb{R}^2 \to \mathbb{R}^3$, smoothly depending on $(u,v) \in \mathbb{R}^2$. Denote by $p(u,v)$ the oriented tangent plane*

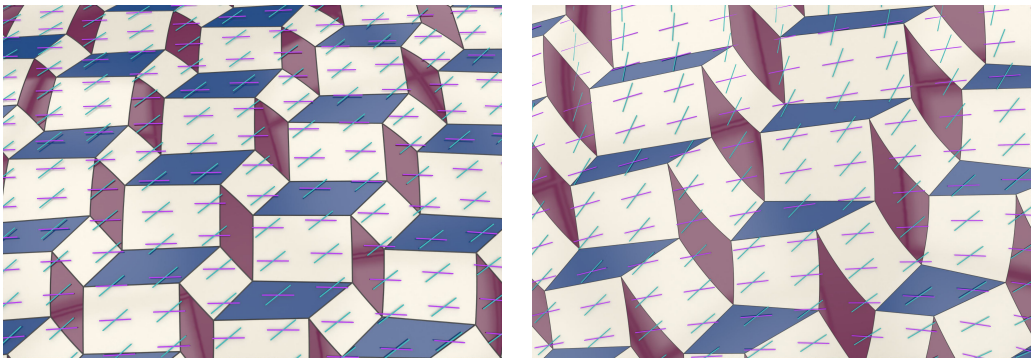

**Figure 9:** The sides of planar quadrilaterals (blue) of an L-net approximating a surface with an attached tangent sphere congruence are aligned with L-conjugate directions (shown in cyan and magenta).

*at a point $f(u,v)$, with the orientation given by the normal $n(u,v)$. We also equip the net with an* ***attached tangent sphere congruence*** *$s : \mathbb{R}^2 \to \mathrm{OrSpheres}(\mathbb{R}^3)$, that is, a map such that $s(u,v)$ is in oriented contact with the oriented tangent plane $p(u,v)$ at each point $f(u,v)$ and the Minkowski lift $S(u,v)$ of $s(u,v)$ is a regular smooth space-like or light-like net in $\mathbb{R}^{3,1}$.*

*The net $f$ is called an* ***L-conjugate net*** *in $\mathbb{R}^3$ with respect to the attached congruence $s$ if the Minkowski lift of $s$ is an L-conjugate net in $\mathbb{R}^{3,1}$ with respect to the Minkowski lift of $p$. In this case, the directions conjugate to $f_u(u,v)$ and $f_v(u,v)$ in the tangent plane $p(u,v)$ of $f$ are called* ***L-conjugate****.*

Beware that $f_u(u,v)$ and $f_v(u,v)$ themselves are not considered L-conjugate with respect to $s$; only their *conjugate directions*, in the ordinary sense, are L-conjugate. In other words, the rulings of the two tangent developables along the isoparameter lines $u = \text{const}$ and $v = \text{const}$ are L-conjugate. Only such a definition of $L$-conjugacy leads to a Laguerre invariant concept. Likewise, the visualization of L-conjugate rulings in the discrete model appears nicely in the edges of each planar face, while discrete parameter lines $u = \text{const}$ and $v = \text{const}$ are actually not directly present in a discrete L-net.

Now, we generalize the notion of L-conjugate directions to an arbitrary parametrization $f(u,v)$.

**Definition 3.10** (L-conjugate tangents)**.** *Two tangent vectors $a \nparallel b$ at a surface point $x = f(u,v) \in \mathbb{R}^3$ are* ***L-conjugate*** *with respect to the attached congruence $s$ if there is a reparametrization $(\bar{f}, \bar{s}) = (f \circ D, s \circ D)$ of $(f, s)$ such that $\bar{f}_u$ is conjugate to $a$, $\bar{f}_v$ is conjugate to $b$, and $\bar{S}_u$ is L-conjugate to $\bar{S}_v$ with respect to $\bar{P}$, where $\bar{S}$ and $\bar{P}$ are the Minkowski lifts of $s \circ D$ and $p \circ D$, respectively.*

We now turn to the analytical formulation of L-conjugacy and prefer to work in a local principal parameterization $f(u,v)$ of the surface. This is sufficient for the geometric understanding and for the application to approximation. With $\kappa_1, \kappa_2$ as principal curvatures of $f$, our parameterization satisfies

$$n_u = -\kappa_1 f_u,\ n_v = -\kappa_2 f_v,\ \langle f_u, f_v \rangle = 0.$$

We are going to consider a single surface point, and assume that at this point,

$$\langle f_u, f_u \rangle = \langle f_v, f_v \rangle = 1.$$

Let the tangent or-sphere $s(u,v)$ have signed radius $r(u,v)$ and center $c_s(u,v) = f + rn$. This defines $S$ and $N$ for the representation in $\mathbb{R}^{3,1}$,

$$S = (c_s, r) = (f + rn, r),\ N = (n, 1).$$

Inserting into (5), we obtain

$$\begin{aligned} L_{S,P,N} &= -\langle f_u, n_u \rangle - r\langle n_u, n_u \rangle = \kappa_1 - r\kappa_1^2, \\ M_{S,P,N} &= -\langle f_u, n_v \rangle - r\langle n_u, n_v \rangle = 0, \\ N_{S,P,N} &= -\langle f_v, n_v \rangle - r\langle n_v, n_v \rangle = \kappa_2 - r\kappa_2^2. \end{aligned} \tag{8}$$

Inserting (8) into (4), we get the condition

$$(\kappa_1 - r\kappa_1^2)a_1b_1 + (\kappa_2 - r\kappa_2^2)a_2b_2 = 0 \tag{9}$$

on two tangent vectors $a_1S_u + a_2S_v$ and $b_1S_u + b_2S_v$ in $\mathbb{R}^{3,1}$ to be L-conjugate.

We now want to express L-conjugacy in the tangent space of $f$, spanned by $f_u, f_v$, following Definition 3.10. By this definition, (9) is equivalent to L-conjugacy of two vectors $\bar{a} = \bar{a}_1 f_u + \bar{a}_2 f_v$ and $\bar{b} = \bar{b}_1 f_u + \bar{b}_2 f_v$ conjugate to $a = a_1 f_u + a_2 f_v$ and $b = b_1 f_u + b_2 f_v$, respectively (because $(S_u, S_v)$ and $(f_u, f_v)$ are transformed in the same way under any reparametrization of $(f, s)$). The vector $\bar{a}$ is related to $a$ via ordinary conjugacy, which is equivalent to vanishing second fundamental form:

$$\kappa_1 a_1 \bar{a}_1 + \kappa_2 a_2 \bar{a}_2 = 0. \tag{10}$$

Rewriting (9) via (10), we get the following expression of L-conjugacy in terms of the *signed principal curvature radii* $\rho_1 := \kappa_1^{-1}$ and $\rho_2 := \kappa_2^{-1}$ of the oriented smooth net $f$ at the point $f(u, v)$.

**Theorem 3.11.** *Consider an orthonormal principal frame $(t_1, t_2, n)$ at a surface point $f(u, v)$. Then, two non-parallel tangent vectors $\bar{a} = \bar{a}_1 t_1 + \bar{a}_2 t_2$ and $\bar{b} = \bar{b}_1 t_1 + \bar{b}_2 t_2$ at $f(u, v)$ are L-conjugate with respect to the congruence $s$, if and only if*

$$(\rho_2 - r)\bar{a}_1\bar{b}_1 + (\rho_1 - r)\bar{a}_2\bar{b}_2 = 0, \tag{11}$$

*where $r$ is the signed radius of the or-sphere $s(u, v)$ and $\rho_1$ and $\rho_2$ are the signed principal curvature radii of $f$ at $f(u, v)$.*

We observe that for $r = 0$, L-conjugacy becomes ordinary conjugacy, and for $r \to \infty$, it becomes orthogonality.

This theorem suggests the following extension of our definition.

**Definition 3.12** (Self-L-conjugate tangents)**.** *With the notation of Theorem 3.11, the tangent vector $\bar{a}$ is called **L-conjugate** to itself with respect to $s$ if $(\rho_2 - r)\bar{a}_1^2 + (\rho_1 - r)\bar{a}_2^2 = 0$.*

Equation (11) implies the following properties of the principal curvature directions in the context of L-conjugacy.

**Corollary 3.13.** *The principal tangents at a surface point $f(u, v)$ are the only orthogonal L-conjugate tangents with respect to $s(u, v)$. They are also the only ones that are simultaneously L-conjugate with respect to two attached sphere congruences that have different sphere radii at the point.*

**Remark 3.14.** *Recall that in the previous definitions, umbilic points were excluded. However, the notion of L-conjugacy can be easily extended to this case via (11). In this case, (11) reduces to $(\rho - r)(\bar{a}_1\bar{b}_1 + \bar{a}_2\bar{b}_2) = 0$, where $\rho := \rho_1 = \rho_2$. If $r \neq \rho$, this forces $\bar{a} \perp \bar{b}$, so every pair of orthogonal directions is L-conjugate. If $r = \rho$, the equation is satisfied for all directions, meaning every direction is L-conjugate to every other.*

**Remark 3.15.** *Equation (9) relates the tangents of contact curves of iso-parameter channel surfaces or equivalently iso-parameter tangent developable surfaces with the base surface $f$ in an L-conjugate parametrization $f(\lambda, \mu)$, i.e., the smooth limit of an L-net approximating $f$. This is useful for the initialization of an approximating L-net, if one wants to base it on an initial selection of the discrete contact curves; see Sec. 5.*

We conclude this section with the following informal description of L-conjugate tangents (for which we do not specify the required non-degeneracy assumptions): Given a curve $c$ on the surface $f$, consider the developable surface $\Delta$ defined as envelope of tangent or-planes of $f$ along $c$, and the channel surface $\Sigma$ defined as envelope of or-spheres of $s$ along $c$ (Fig. 8). Then, at each point of $c$, the ruling of $\Delta$ is L-conjugate to that principal tangent of $\Sigma$ which is orthogonal to its characteristic circle. Cf. Fig. 10.

A side remark is that the surface $f$ together with its unit normal field defines a Legendre immersion (Musso and Nicolodi, 2018); thus, our setup corresponds to a Legendre immersion with a choice of sphere at each contact element, given by the attached sphere congruence.

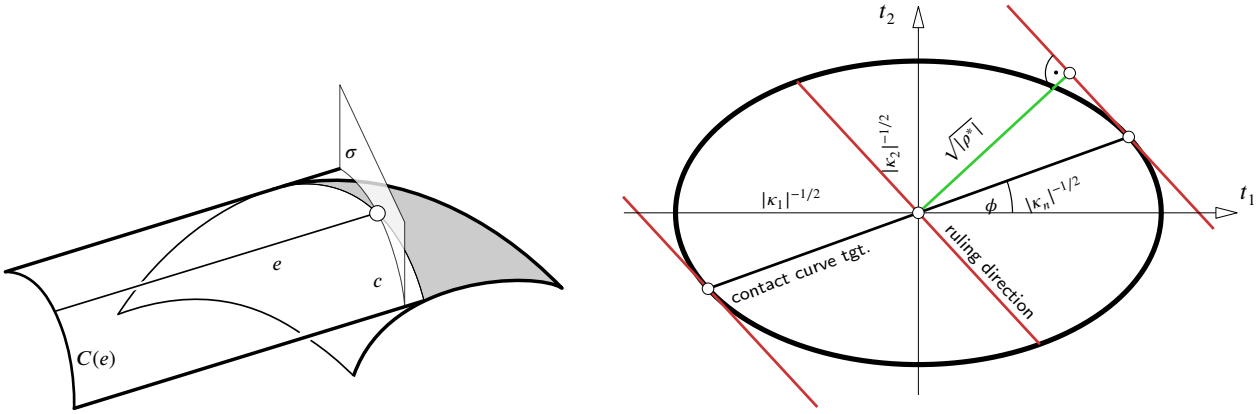


**Figure 10:** Left: A cylinder $C(e)$ which is tangent to a given surface along a curve defines along its ruling $e$ a dual curvature radius $\rho^*$. It is the signed curvature radius of the intersection curve $c$ with a plane $\sigma$ orthogonal to $e$. Right: The Dupin indicatrix at a surface point visualizes the normal curvatures as distances $|\kappa_n|^{-1/2}$ of its points from the center (contact point), and dual curvature radii via distances $\sqrt{|\rho^*|}$ of its tangents from the center. The parallel tangents are the Dupin indicatrix of the right circular cylinder that is in 2nd order contact with the cylinder $C(e)$ along $e$. Images taken from (Pellis et al., 2020).

## 4. L-conjugacy and dual curvature radii of a surface with respect to a tangent sphere congruence

In this section, we discuss informally the close relation of the L-conjugacy relation (11) to a dual viewpoint of surface theory that is based on oriented tangent planes rather than points. In particular, there is a relation to dual curvature radii which are a dual counterpart to normal curvatures. We also discuss the various instances of self-L-conjugate (L-asymptotic) directions (Sec. 4.1). This is relevant for approximation, since we need to avoid L-asymptotic directions. Despite that, we briefly study L-asymptotic parameterizations in Sec. 4.2, mainly due to the appearance of a Laguerre-geometric formulation of principal symmetric nets introduced in (Pellis et al., 2020). Finally, we address important special cases of attached sphere congruences (Sec. 4.3) that are used in Sec. 5, where we then discuss approximation with L-nets.

### 4.1. Classification of contact elements of a surface with respect to an attached sphere congruence

*Dual curvature radii* Let us briefly summarize some basic facts on the mentioned dual viewpoint of surface theory in Euclidean 3-space. We view a surface $f(u,v)$ as set of oriented tangent planes $p(u,v)$ and instead of curves on $f$ we consider developable surfaces enveloped by one-parameter families of tangent planes $p$. At a given surface point $f(u,v)$ we consider a tangent $e$ and the cylinder $C(e)$ enveloped by those or-planes $p$ of $f$ that are parallel to $e$. In other words, $C(e)$ has rulings parallel to $e$ and is tangent to $f$ along a curve (see Fig. 10). The dual curvature radius $\rho^*(e)$ to the ruling direction $e$ is defined as curvature radius (inverse normal curvature) of the cylinder $C(e)$ in direction orthogonal to $e$. It is the signed radius of a right circular cylinder that is in 2nd order contact with $C(e)$ along the ruling $e$.

Fig. 10 illustrates this at hand of the Dupin indicatrix at $f(u,v)$, which visualizes normal curvatures $\kappa_n(\phi)$ for tangents that form the angle $\phi$ with the first principal tangent $t_1$. It is a radial diagram of $|\kappa_n(\phi)|^{-1/2}$ and also visualizes dual curvature radii as explained in Fig. 10.

Normal curvatures $\kappa_n(\phi)$ at a surface point satisfy Euler's formula

$$\kappa_n(\phi) = \kappa_1 \cos^2\phi + \kappa_2 \sin^2\phi.$$

Its dual is Blaschke's formula for the dual curvature radius to the ruling direction $t_1 \cos\phi_e + t_2 \sin\phi_e$,

$$\rho^*(\phi_e) = \rho_2 \cos^2\phi_e + \rho_1 \sin^2\phi_e, \tag{12}$$

where $\rho_1 := \kappa_1^{-1}$ and $\rho_2 := \kappa_2^{-1}$ are the signed principal curvature radii of $f$ (Pellis et al., 2020, Proposition 2.8).

*Self-L-conjugate tangents* According to Definition 3.12, a tangent vector $\bar{a} = t_1 \cos\phi_e + t_2 \sin\phi_e$ is L-conjugate to itself with respect to an attached tangent sphere congruence $s$, if and only if

$$(\rho_2 - r)\cos^2\phi_e + (\rho_1 - r)\sin^2\phi_e = 0, \tag{13}$$

which, by (12), expresses a vanishing difference $\rho^*(\phi_e) - r$ of dual curvature radius and sphere radius. These tangents are called *L-asymptotic with respect to s*. They are real for $(\rho_1 - r)(\rho_2 - r) < 0$ and symmetric with respect to the principal directions, with which they form the angle $\phi_a$ given by

$$\tan\phi_a = \pm\sqrt{-\frac{\rho_2 - r}{\rho_1 - r}}. \tag{14}$$

L-asymptotic tangents are fixed elements in the involutory projective map between L-conjugate tangents at a surface point.

*L-characteristic tangents* L-conjugate tangents that are reflection-symmetric with respect to the principal directions are called *L-characteristic tangents*. Their angles $\pm\phi_c$ against the first principal direction are computed via

$$\tan\phi_c = \pm\sqrt{\frac{\rho_2 - r}{\rho_1 - r}}, \tag{15}$$

where we applied (11) for $(a_1, a_2) = (b_1, -b_2) = (\cos\phi_c, \sin\phi_c)$. These directions are real for $(\rho_1 - r)(\rho_2 - r) > 0$.

Just as we distinguish between hyperbolic, parabolic, elliptic, and flat points in elementary surface theory, we have an analogous classification here. To make it even more transparent, motivated by (13), we define *dual curvature radii* $\rho_s^*$ *of a surface* $f$ *with respect to an attached sphere congruence* $s$ as

$$\rho_s^* := \rho^* - r. \tag{16}$$

Clearly, these dual curvature radii with respect to $s$ satisfy a generalized Blaschke formula

$$\rho_s^*(\phi_e) = (\rho_2 - r)\cos^2\phi_e + (\rho_1 - r)\sin^2\phi_e = \rho_{s,1}^*\cos^2\phi_e + \rho_{s,2}^*\sin^2\phi_e. \tag{17}$$

Note that the dual curvature radii $\rho_{s,1}^*, \rho_{s,2}^*$ with respect to $s$ for rulings in first and second principal directions are

$$\rho_{s,1}^* = \rho_2 - r,\ \rho_{s,2}^* = \rho_1 - r.$$

Introduce the value

$$\Lambda := \rho_{s,1}^*\rho_{s,2}^*.$$

It is more natural to speak of *contact elements* of the oriented surface (that is, pairs $(f(u,v), p(u,v))$ consisting of a surface point and the oriented tangent plane at the point), rather than surface points, because Laguerre transformations naturally act on contact elements rather than points.

We can now formulate the classification of surface contact elements with respect to an attached sphere congruence:

**L-hyperbolic contact element ($\Lambda < 0$):** two real L-asymptotic tangents are characterized by (14).

**L-parabolic contact element ($\Lambda = 0$ and exactly one $\rho_{s,i}^* \neq 0$):** a single L-asymptotic tangent that is also principal; any tangent direction is L-conjugate to that direction.

**L-elliptic contact element ($\Lambda > 0$):** no real L-asymptotic tangent, but a pair of principal symmetric and L-conjugate tangents given by (15).

**L-flat contact element ($\rho_{s,1}^* = \rho_{s,2}^* = 0$):** the congruence sphere is in second order contact with $f$. This is only possible at umbilic points, which were excluded in our previous discussion; however, the notion of L-conjugacy can be easily extended to this case via (11).

### 4.2. L-asymptotic developables and L-asymptotic parameterizations

Since points are not preserved under Laguerre transformations, the same is true for curves on surfaces. Instead of integrating special directions such as principal directions or asymptotic directions to curves and further to isoparameter curves of special parameterizations, we now have to view tangents as rulings of developable surfaces that are tangent to $f$. We call them *tangent developables*. Recall that $f$ has no parabolic and umbilic points.

For principal tangents, this is simple. A principal developable is just a developable surface that is tangent to $f$ along a principal curvature line. If the curvature line follows the first principal directions, the rulings of the principal developable are orthogonal to them and thus parallel to the second principal direction. The arising principal parameterizations constitute orthogonal smooth L-conjugate nets.

We now focus on L-asymptotic tangents (rulings) $e_a$ and integrate them to *L-asymptotic developables*. The tangents of their contact curves with $f$ are conjugate to the rulings $e_a$ in the usual sense, given by equation (10). At each ruling of an L-asymptotic developable, the radius $r$ of the sphere of the congruence equals the dual curvature radius $\rho^*$ of the ruling $e_a$. This sphere of radius $\rho^*$ is known as *Mannheim sphere* (Blaschke and Leichtweiß, 1973) and is a dual counterpart to the well-known Meusnier sphere (Blaschke and Leichtweiß, 1973). While the latter contains the osculating circles of all surface curves through a given line element, the Mannheim sphere is enveloped by all oriented rotational cones $\Gamma(e_a)$ which share the ruling $e_a$, have their vertex $v_c$ on $e_a$ and are in second order plane contact with $f$. Such an osculating cone $\Gamma(e_a)$ can be constructed as follows: All tangent planes of $f$ through $v_c$ envelope a general cone and $\Gamma(e_a)$ is in second order contact with that cone along the entire ruling $e_a$ (see Fig. 7 in (Pellis et al., 2020)).

An *L-asymptotic parameterization* is a parameterization $f(u, v)$ such that the isoparameter tangent developables are L-asymptotic developables. The rulings of the developables are symmetric with respect to the principal directions and at each contact element, the common Mannheim sphere of the two isoparameter developables equals the congruence sphere $s(u, v)$. This is related to smooth asymptotic parameterizations, where the common osculating plane of the isoparameter curves equals the tangent plane of the surface. An L-asymptotic parameterization is the same as a smooth $S^*$-net introduced in (Pellis et al., 2020).

In the cyclographic model, the sphere congruence $s(u, v)$ appears as a surface $S(u, v) \subset \mathbb{R}^{3,1}$, such that all isoparameter curves have osculating planes that lie in the attached isotropic tangent hyperplanes $P(u, v)$. Indeed, since the tangents of isoparameter lines are self-L-conjugate, by (4), we get $L_P = N_P = 0$. By (6) and (5), this is equivalent to $\langle\langle S_u, N\rangle\rangle = \langle\langle S_{uu}, N\rangle\rangle = 0$ and $\langle\langle S_v, N\rangle\rangle = \langle\langle S_{vv}, N\rangle\rangle = 0$, which means that the osculating planes of the isoparameter curves lie in the attached isotropic hyperplanes.

Three consecutive or-planes in a discrete model of a developable surface determine an or-cone which is in oriented contact with them. It is the discrete version of the osculating cone. This leads to the discrete versions of L-asymptotic parameterizations. They are not L-nets, but counterparts to the well-studied A-nets (Bobenko and Suris, 2008). One can view them as nets of or-planes, where we obtain exactly the discrete $S^*$-nets of (Pellis et al., 2020), or as nets of or-spheres, with the following characterization:

*A discrete L-asymptotic parameterization is a net of or-planes such that each or-plane $p_{ij}$ and its four neighbors $p_{i-1,j}$, $p_{i+1,j}$, $p_{i,j-1}$, $p_{i,j+1}$, are in or-contact to a common or-sphere $s_{ij}$. Viewing the structure as a net of or-spheres, each or-sphere $s_{ij}$ and its four neighbors $s_{i-1,j}$, $s_{i+1,j}$, $s_{i,j-1}$, $s_{i,j+1}$, are in or-contact to a common or-plane.*

Especially the second formulation is an obvious generalization of discrete A-nets; there, the spheres are points.

### 4.3. Important special cases of attached sphere congruences

*Constant sphere radius* We start the discussion with a discrete L-net with constant signed radius $r$. At a plane $p_{ij}$ of the L-net, we have four or-spheres of the same radius that are tangent to $p_{ij}$. Thus, the centers of the four spheres lie in a plane that is parallel to $p_{ij}$ and at signed distance $r$. This is the same as an offset of a Q-net. Clearly, all edge cones are cylinders of radius $|r|$. Even in this simple case, our optimization approach can be preferable to working with the offset directly, as it can avoid singularities and improve approximation.

*Congruence of mid spheres* The mid sphere $s_m$ of a surface $f$ at a contact element is the tangent or-sphere whose center is the midpoint of the principal curvature centers. Hence, its radius equals $r_m = (\rho_1 + \rho_2)/2$. Being an average of the principal spheres, the mid sphere provides a good local approximation of $f$. Moreover, like the principal spheres, mid spheres are a concept of Laguerre geometry. A Laguerre transformation maps mid spheres to mid spheres, in general changing their radii.

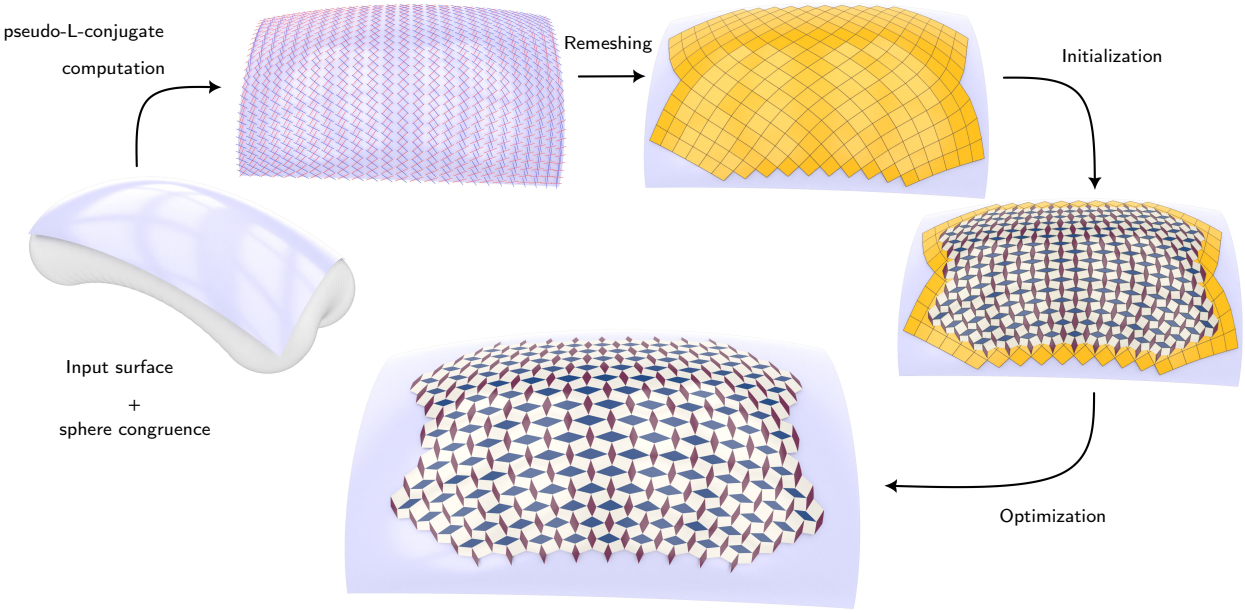


**Figure 11:** Algorithm flow. Starting from an input surface with an attached sphere congruence, we compute pseudo-L-conjugate directions and remesh along these directions to obtain a quad mesh. We then initialize the L-net using planes at the vertices of the quad mesh, and refine it through a final optimization step.

If we attach the congruence of mid spheres $s_m(u, v)$ to a surface $f$, we obtain as dual principal curvature radii with respect to $s_m$,

$$\rho^*_{s,1} = \rho_2 - r_m = \frac{\rho_2 - \rho_1}{2}, \qquad \rho^*_{s,2} = \rho_1 - r_m = \frac{\rho_1 - \rho_2}{2}.$$

At non-umbilic points, we have $\Lambda < 0$ and thus *all contact elements are L-hyperbolic*. Due to (14), $\phi_a = \pm\pi/4$, hence the *L-asymptotic tangents are orthogonal, bisecting the principal tangents*. L-conjugacy (11) simplifies to

$$\bar{a}_1\bar{b}_1 - \bar{a}_2\bar{b}_2 = 0. \tag{18}$$

This expresses symmetry with respect to the L-asymptotic tangents. We see here relations to Euclidean minimal surfaces, which appear as that special case where the mid spheres have radius zero and are the points of $f$. This is also the case in which L-conjugacy is the same as ordinary conjugacy.

Using the attached congruence of mid spheres, we have frame fields of L-conjugate directions with a constant angle. They may provide interesting alternatives to the principal directions.

*Surfaces with only L-parabolic contact elements* At an L-parabolic point, one principal curvature radius equals the radius $r$ of the congruence sphere. Hence, every surface $f$ has only L-parabolic contact elements if we attach to it a congruence of principal spheres, say, the ones with radius $\rho_1$. Then, any direction is L-conjugate to the second principal direction. This can provide interesting types of flexibility for approximation and deserves further study.

## 5. Surface approximation with L-nets

To approximate a surface with an L-net, we start with an input surface $f$ of positive Gaussian curvature and a signed radius function $r$, both defined on the same parameter domain and represented as tensor product B-splines.

An overview of our approach is as follows: We use the B-spline representation to compute a smooth L-conjugate direction field over sampled surface points. This direction field guides a quad remeshing procedure, leading to a quadrilateral mesh aligned with the L-conjugate directions. This aligned quad mesh serves as the initialization for our L-net construction algorithm. Finally, we refine the initial approximate L-net through numerical optimization using

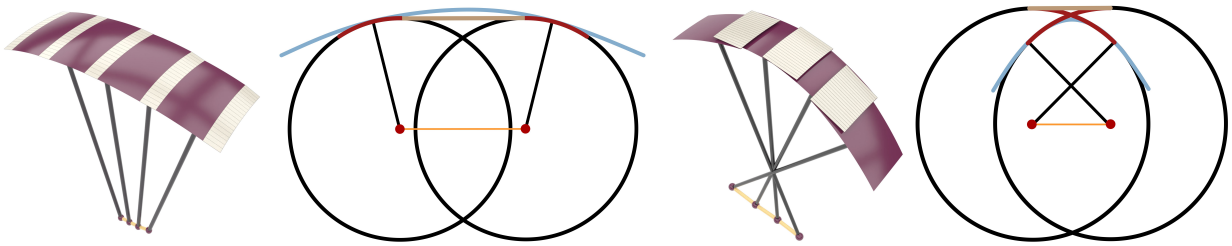

**Figure 12:** Spherical panels strips of an L-net aligned with the principal directions and their 2D counterparts. Black lines connect contact points on the approximated surface/curve to the sphere/circle centers, shown as red dots, which are joined by orange lines. In the 2D diagrams, brown lines represent common tangent lines of both circles (the 2D counterparts of edge cones), red arcs correspond to the 2D counterparts of spherical panels, and light-blue curves represent the approximated curve. (Left) A radius function within the safe range produces a smooth strip of spherical panels and cone strips; (Right) A radius function $r > \min\{\rho_1, \rho_2\}$ produces swallowtail singularities.

the Levenberg-Marquardt (Marquardt, 1963) algorithm to fulfill the constraints for an L-net with high accuracy while maintaining close proximity to the reference surface and fairness (Fig. 11).

## 5.1. Computation of L-conjugate directions

*Principal frames* The input surface $f(\lambda, \mu)$ is represented as a tensor product B-spline surface. At each sample point $f(\lambda_i, \mu_j)$, we compute a principal frame $(t_1, t_2, n)$ and signed principal curvature radii $\rho_1$ and $\rho_2$, where $\lambda_i$ and $\mu_j$ are obtained by uniform subdivision of the $\lambda$ and $\mu$ parameter domains. We choose $n$ inward-pointing, so that $\rho_1, \rho_2 \geq 0$.

*Signed-radius function* The attached sphere congruence is represented by the signed radius function $r$. For reasonable approximation of the given surface, we require it to be positive. In the discrete setting, the choice of radius affects the overall appearance of the approximation. In particular, when approximating a surface $f$, singularities emerge when the sphere radii exceed the radii of the principal curvature spheres at the corresponding contact points. Specifically, if the sphere radius satisfies $r > \min\{\rho_1, \rho_2\}$, swallow-tail singularities (containing regression curves) appear. For aesthetically pleasing approximations, we use $r < \min\{\rho_1, \rho_2\}$. See Fig. 12.

*L-conjugate directions* For our initialization algorithm, we consider a discrete version of the net of contact curves of isoparameter tangent developable surfaces in a smooth L-conjugate net defined on $f$. Equivalently, this curve net is formed by the contact curves of isoparameter channel surfaces in the attached sphere congruence. This is not fully Laguerre-geometric, but turned out to be easier to implement than the plane-based definition of L-conjugate directions. Thus, we are not initially computing L-conjugate directions, but directions that satisfy equation (9) (cf. Remark 3.15). We call them *pseudo-L-conjugate*. For their computation, we first prescribe one direction by specifying an angle $\theta$ against the first principal direction $t_1$. This angle is a design parameter (see Fig. 13). It may be set as a constant across all sampled points, or it can be defined as an angle field varying over $f$. However, a smoothly varying angle field is required to arrive at a proper discrete version of a smooth L-net. The second direction is computed by solving equation (9). In this way, we obtain a pseudo-L-conjugate frame field. We point out that the actual initialization of the L-net, as explained below, indeed respects the associated L-conjugate frame field, which is seen in the sides of the planar quadrilaterals (see Fig. 9).

## 5.2. Quad remeshing and initialization

*Quad remeshing* Once the frame field is computed, we proceed with an anisotropic quad remeshing procedure implemented in the igl library (Jacobson, Panozzo et al., 2018), where LibQEx (Ebke, Bommes, Campen and Kobbelt, 2013) is used to extract the quad mesh when singularities are present. The extracted quad mesh $Q$ has edges aligned with the directions of the frame field.

*Initialization* To initialize an L-net, we can interpret the vertices of $Q$ as contact points of oriented tangent planes or as contact points of tangent oriented spheres.

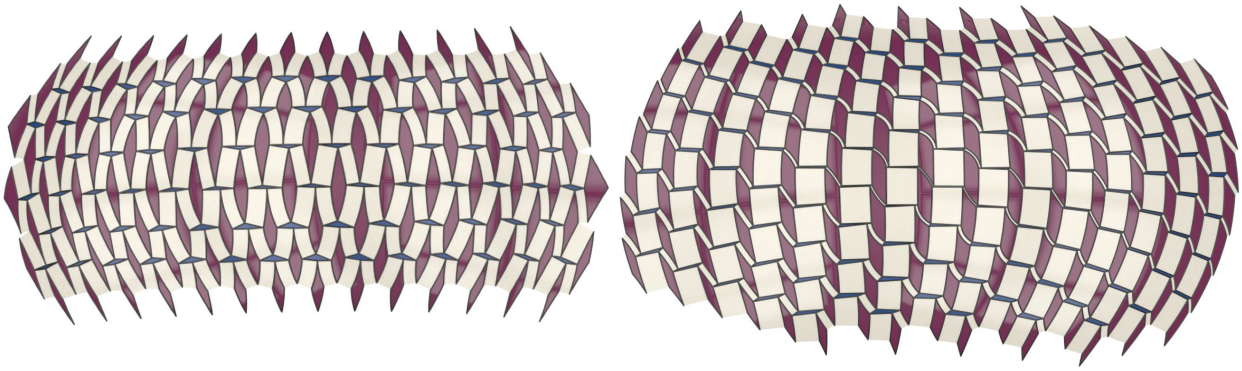

**Figure 13:** Two L-nets constructed from the same attached sphere congruence but with different initial L-conjugate directions. The initialization angle $\theta$ between the first L-conjugate direction and the first principal direction is set to constant value $\theta = \pi/3$ (left) and $\theta = \pi/6$ (right).

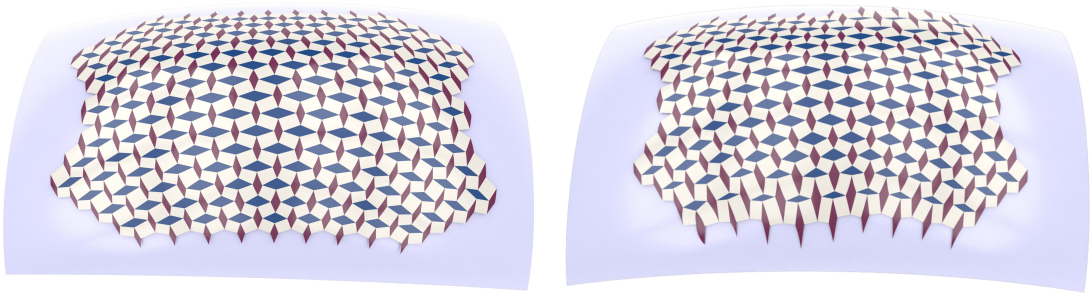

**Figure 14:** L-nets initialized interpreting vertices of the quad mesh $Q$ as contact points of oriented tangent planes (left) and tangent oriented spheres (right).

The first approach, placing planes at the vertices of $Q$, preserves the mesh extent near the boundary: when initializing with or-spheres instead, the boundary spheres are not used for panel generation, resulting in a shrunken L-net. However, the differences are visually negligible (see Fig. 14). Following the first interpretation, our L-net $L = (\mathcal{V}_\mathcal{S}, \mathcal{E}_\mathcal{C}, \mathcal{F}_\mathcal{P})$ is computed as follows: (i) $Q$ and $L$ have dual combinatorics, so for each vertex $v_i \in Q$, the corresponding plane $p_i \in \mathcal{F}_\mathcal{P}$ is the plane with normal $n_i$ (the normal of the reference surface $f$ at vertex $v_i$) and signed distance from the origin $h_i = -\langle v_i, n_i \rangle$; (ii) for each quad $q \in Q$, we define an initial sphere $s_f = (c_f, r_f)$ by projecting the barycenter of $q$ onto the reference surface as $b_q = f(\lambda_q, \mu_q)$; the radius of the sphere is $r_f = r(\lambda_q, \mu_q)$ and its center is $c_f = b_q + r_f n(\lambda_q, \mu_q)$; (iii) we compute the cone strip for each pair of adjacent spheres. In general, this initial configuration is not an L-net since the spheres and planes are not exactly in oriented contact. However, it provides a good initial guess for the final optimization algorithm to obtain an L-net.

## 5.3. Final optimization

*Variables* In the final optimization, our goal is to approximate $f$ with an L-net $L = (\mathcal{V}_\mathcal{S}, \mathcal{E}_\mathcal{C}, \mathcal{F}_\mathcal{P})$ with high accuracy. The whole structure depends only on the or-spheres $s_{ij} = (c_{ij}, r_{ij}) \in \mathcal{V}_\mathcal{S}$ and or-planes $p_{ij} = (n_{ij}, h_{ij}) \in \mathcal{F}_\mathcal{P}$, so the variables in our Levenberg-Marquardt algorithm are the sphere centers $c_{ij}$, signed radii $r_{ij}$, plane normals $n_{ij}$, and signed distances $h_{ij}$ from the origin. Plane normals are constrained to be unit; we express this by vanishing energy

$$E_{\text{unit}} = \sum_{p_{ij} \in \mathcal{F}_\mathcal{P}} (\|n_{ij}\|^2 - 1)^2. \tag{19}$$

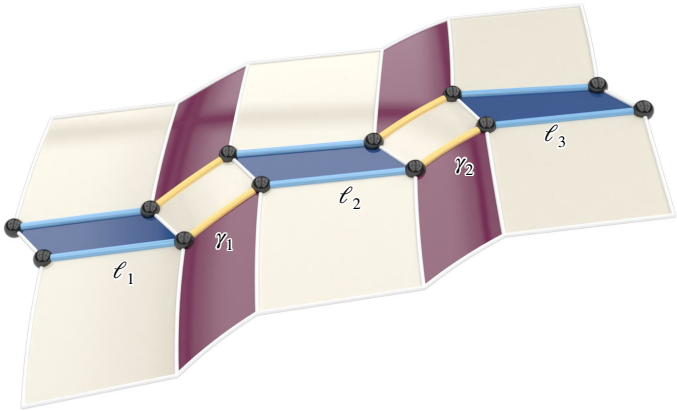


**Figure 15:** Piecewise-smooth curves alternating pattern between (light blue) straight segments $\ell_i$ and (yellow) circular arcs $\gamma_i$ along a strip.

*Oriented contact* We need to ensure that the or-spheres and their neighboring or-planes are in oriented contact. This is expressed by vanishing energy

$$E_{\mathrm{oc}} = \sum_{p_{ij} \in \mathcal{F}_{\mathcal{P}}} \sum_{a,b=0}^{1} \left( \langle c_{i+a,\, j+b}, n_{ij} \rangle + h_{ij} - r_{i+a,\, j+b} \right)^2 . \tag{20}$$

*L-net Fairness* As is well known in optimization, the energy needs to include fairness terms that penalize abrupt changes in the directions of the patch boundaries.

The boundary curves of the elements of an L-net form two families of piecewise-smooth curves (see the orange and green curves in the inset), each consisting of alternating straight line segments and circular arcs meeting at the contact points between or-spheres and or-planes. They follow the pattern $\ell_1, \gamma_1, \ell_2, \gamma_2, \ldots$, where $\ell_i$ denotes a straight segment and $\gamma_i$ a circular arc (Fig. 15). To preserve the structure of L-nets, we impose constraints independently on each subsequence: consecutive straight segments $\ell_i, \ell_{i+1}$ are constrained regardless of the arc $\gamma_i$ between them, and similarly for consecutive arcs $\gamma_i, \gamma_{i+1}$.

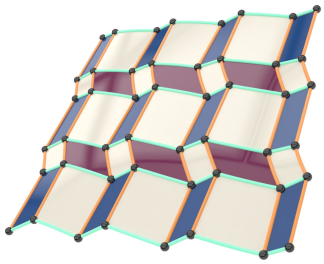

Aiming at an appropriate fairness term for the piecewise smooth curves, we first need to express their vertices. To constrain the straight segments, we consider three consecutive or-spheres $s_i, s_j, s_k$ of signed radii $r_i, r_j, r_k$ and or-planes $p_0, p_1, p_2, p_3$ with normals $n_0, n_1, n_2, n_3$, where $p_0, p_3$ are in oriented contact with $s_i, s_j$ and $p_1, p_2$ are in oriented contact with $s_j, s_k$ (see Fig. 16, left). In this arrangement, we have two pairs of consecutive straight segments $\ell_i = (a_0, a_1)$, $\ell_{i+1} = (a_2, a_3)$, $\bar{\ell}_i = (b_0, b_1)$, and $\bar{\ell}_{i+1} = (b_2, b_3)$ with the endpoints at the contact points between the or-spheres and or-planes:

$$\begin{aligned} a_0 &= c_i - r_i n_0, & b_0 &= c_i - r_i n_3, \\ a_1 &= c_j - r_j n_0, & b_1 &= c_j - r_j n_3, \\ a_2 &= c_j - r_j n_1, & b_2 &= c_j - r_j n_2, \\ a_3 &= c_k - r_k n_1, & b_3 &= c_k - r_k n_2. \end{aligned}$$

These segments are sides of the quadrilateral faces contained in the planes $p_0$, $p_1$, $p_3$, and $p_2$, respectively. The fairness term for straight segments is based on the idea that vectors $a_1 - a_0$ and $a_3 - a_2$ should be close to each other, and

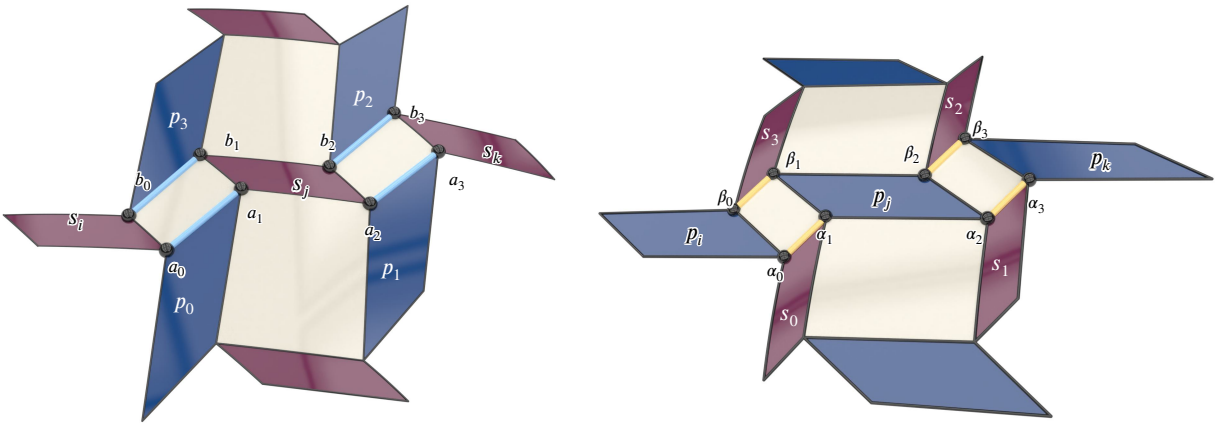


**Figure 16:** The notation for the fairness energy terms $E_{\ell\text{fair}}$ (left) and $E_{\gamma\text{fair}}$ (right).

likewise for the $b$'s. This is expressed by a small value of the energy

$$E_{\ell\text{fair}} = \sum_{s_i, s_j, s_k \text{ consecutive}} \left( \|a_1 - a_0 - a_3 + a_2\|^2 + \|b_1 - b_0 - b_3 + b_2\|^2 \right). \tag{21}$$

This energy is well-defined even if the or-planes and or-spheres are not exactly in oriented contact, and its choice is motivated by the discrete approximation of gradually changing rulings.

To constrain the circular arcs, we proceed in the same way. Consider three consecutive or-planes $p_i, p_j, p_k$ and or-spheres $s_0, s_1, s_2, s_3$, where $s_0, s_3$ are in oriented contact with $p_i, p_j$ and $s_1, s_2$ are in oriented contact with $p_j, p_k$ (see Fig. 16, right). In this arrangement, we have two pairs of consecutive circular arcs $\gamma_i = (\alpha_0, \alpha_1)$, $\gamma_{i+1} = (\alpha_2, \alpha_3)$, $\bar{\gamma}_i = (\beta_0, \beta_1)$, and $\bar{\gamma}_{i+1} = (\beta_2, \beta_3)$ with the endpoints

$$\begin{aligned} \alpha_0 &= c_0 - r_0 n_i, & \beta_0 &= c_3 - r_3 n_i, \\ \alpha_1 &= c_0 - r_0 n_j, & \beta_1 &= c_3 - r_3 n_j, \\ \alpha_2 &= c_1 - r_1 n_j, & \beta_2 &= c_2 - r_2 n_j, \\ \alpha_3 &= c_1 - r_1 n_k, & \beta_3 &= c_2 - r_2 n_k. \end{aligned}$$

These arcs are some of the boundary curves of the spherical panels $s_0$, $s_1$, $s_3$, and $s_2$. The fairness term for circular arcs is expressed by a small value of the energy

$$E_{\gamma\text{fair}} = \sum_{p_i, p_j, p_k \text{ consecutive}} \left( \|\alpha_1 - \alpha_0 - \alpha_3 + \alpha_2\|^2 + \|\beta_1 - \beta_0 - \beta_3 + \beta_2\|^2 \right). \tag{22}$$

*Proximity Energies* To ensure that the L-net approximates the reference surface $f$, we include terms that express the proximity of the plane-sphere contact points in the L-net to the surface $f$. For each contact point $x$ in $L$, we denote by $x_f$ its closest-point projection onto $f$ and denote by $n_f$ the surface normal at $x_f$. We express the proximity in terms of the distance to the projected point $x_f$ and the distance to the tangent plane of the reference surface $f$ at $x_f$,

$$E_{\text{prox}} = \sum_x \|x - x_f\|^2, \quad E_{\text{tan}} = \sum_x \langle x - x_f, n_f \rangle^2. \tag{23}$$

*Tangential distance* For visual appearance and design purposes, it may be desirable for the spherical panels to be larger than the conical and planar quads. This can be addressed by minimizing the width of the cone strips connecting adjacent spheres. The width equals the tangential distance between two or-spheres $s_i$ and $s_j$, and is computed as $d_{tang}(s_i, s_j) = \sqrt{\|c_i - c_j\|^2 - (r_i - r_j)^2}$. We introduce the following energy term to minimize the tangential distance over all pairs of adjacent or-spheres of the L-net:

$$E_{\text{td}} = \sum_{s_i, s_j \text{ adjacent}} \left( \|c_i - c_j\|^2 - (r_i - r_j)^2 \right)^2. \tag{24}$$

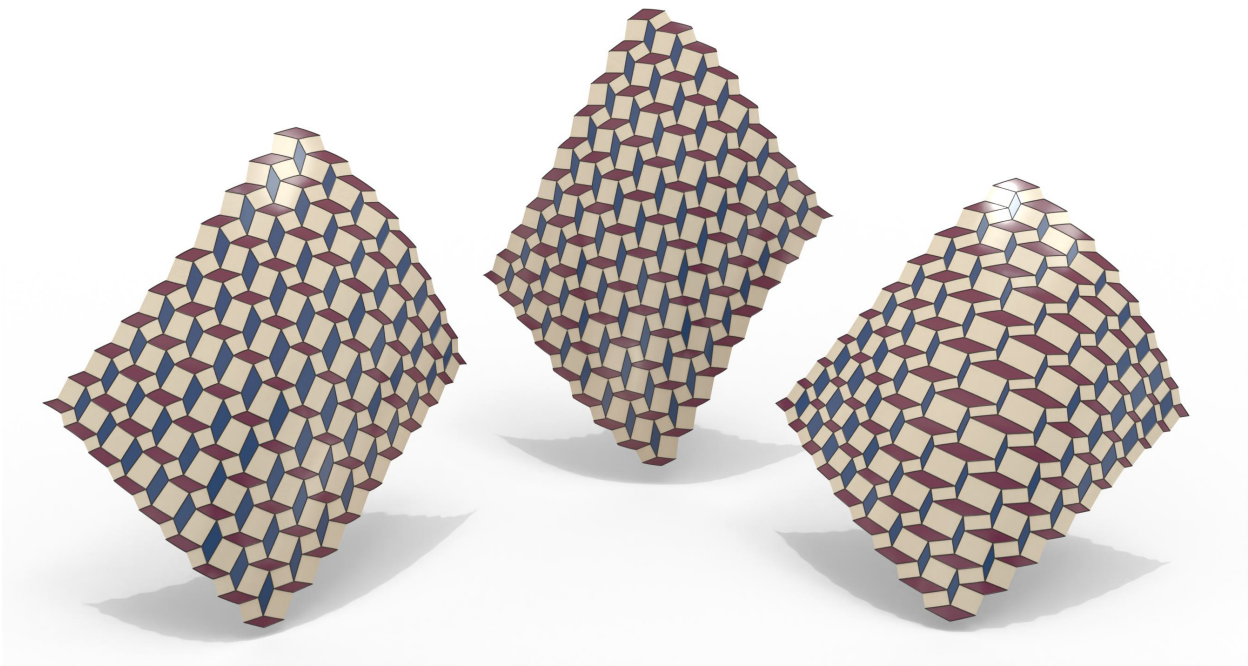

**Figure 17:** (Mid) L-mesh initialization using L-conjugate directions computed using $\theta(u, v) = \pi/4$ for the first direction and multiplier factor for the signed radius function $\tau = 0.75$. (Left) Final optimization without tangential distance minimization. (Right) Final optimization with tangential distance minimization.

*Optimization* We also include the standard Levenberg-Marquardt regularization term $E_{\text{reg}} = \|X - X^{\text{prev}}\|^2$ to avoid abrupt changes during the optimization. Here $X$ is the vector of all variables and $X^{\text{prev}}$ contains their values from the previous iteration. Combining all energy terms with their corresponding weights yields the total energy

$$E = \omega_{\text{oc}} E_{\text{oc}} + \omega_{\gamma\text{fair}} E_{\gamma\text{fair}} + \omega_{\ell\text{fair}} E_{\ell\text{fair}} + \omega_{\text{prox}} E_{\text{prox}} + \omega_{\text{tan}} E_{\text{tan}} + \omega_{\text{td}} E_{\text{td}} + \omega_{\text{reg}} E_{\text{reg}} + \omega_{\text{unit}} E_{\text{unit}}. \tag{25}$$

All examples were computed with $\omega_{\text{reg}} = 10^{-4}$, $\omega_{\ell\text{fair}} = 10^{-3}$, $\omega_{\gamma\text{fair}} = 10^{-3}$, $\omega_{\text{unit}} = 10$, and $\omega_{\text{oc}} = 1$, where the only modifications appear on the proximity terms, and whether we include the tangential distance minimization term or not (see Fig. 17). Both fairness energies $\omega_{\ell\text{fair}}$ and $\omega_{\gamma\text{fair}}$ are multiplied by 0.1 every ten steps to decrease the influence of these terms. After a certain number of iterations or convergence, we run 20 additional optimization steps with all weights set to zero except for $\omega_{oc}$ and $\omega_{unit}$. The resulting change in the L-net is minimal, but this final pass ensures that all elements satisfy the oriented contact constraints close to machine precision. It also addresses the fact that fairness energies, which should just be small but in general not vanish, do not fight against the hard contact constraints.

## 6. Results, discussion, and future research

For our results, we define a signed radius function $r(u, v) = \tau \cdot \min\{\rho_1, \rho_2\}$, with $\tau \in (0, 1)$ ensuring that the sphere radius remains strictly below the smallest principal curvature radius, avoiding swallow-tail singularities.

The first direction of the L-conjugate pair is initialized via a function $\theta(u, v) \in [0, \pi/2]$, representing the angle of the direction against the first principal direction. We consider three types of initialization:

- *Constant:* $\theta_C(u, v) = c$, for some $c \in [0, \pi/2]$.
- *Linear:* along the $u$- and $v$-directions, respectively,

$$\theta^{\theta_{max}}_{\theta_{min}}(u) = (1 - u)\,\theta_{min} + u\,\theta_{max}, \tag{26}$$

$$\theta^{\theta_{max}}_{\theta_{min}}(v) = (1 - v)\,\theta_{min} + v\,\theta_{max}. \tag{27}$$

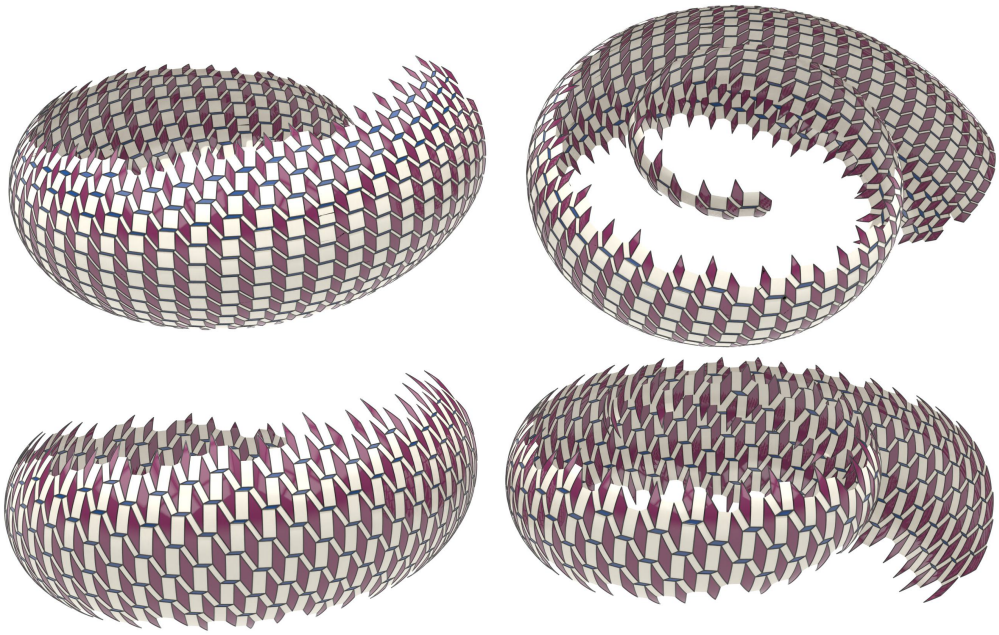

**Figure 18:** Spiral L-net designs obtained with different initializations. (Top) $\tau = 0.90$, $\theta_{\cos}^{(0,\pi/2)}(u)$; (bottom) $\tau = 0.95$, $\theta_C = \pi/4$.

| Fig | $\tau$ | $\theta(u,v)$ | $\omega_{\text{prox}}$ | $\omega_{\tan}$ | $\omega_{\text{td}}$ | T(ms)/iter | iter | Residual | Residual $E_{\text{oc}}$ |
|---|---|---|---|---|---|---|---|---|---|
| 3 | 0.90 | $\theta_C = 5\pi/12$ | $10^{-4}$ | $10^{-4}$ | $10^{-3}$ | 446.9 | 100 | $2.08 \cdot 10^{-7}$ | $8.94 \cdot 10^{-18}$ |
| 4 | 0.75 | $\theta_C = \pi/4$ | $10^{-4}$ | $10^{-4}$ | $10^{-5}$ | 84.1 | 100 | $3.30 \cdot 10^{-5}$ | $1.61 \cdot 10^{-26}$ |
| 13 (left) | 0.94 | $\theta_C = \pi/3$ | $10^{-4}$ | $10^{-4}$ | 0 | 10.5 | 150 | $4.75 \cdot 10^{-8}$ | $8.41 \cdot 10^{-28}$ |
| 13 (right) | 0.94 | $\theta_C = \pi/6$ | $10^{-2}$ | $10^{-2}$ | 0 | 13.9 | 150 | $1.97 \cdot 10^{-7}$ | $1.52 \cdot 10^{-27}$ |
| 17 (left) | 0.75 | $\theta_C = \pi/6$ | $10^{-4}$ | $10^{-4}$ | 0 | 7.4 | 200 | $5.30 \cdot 10^{-9}$ | $1.93 \cdot 10^{-28}$ |
| 17 (right) | 0.75 | $\theta_C = \pi/6$ | $10^{-4}$ | $10^{-4}$ | $10^{-3}$ | 8.4 | 200 | $7.62 \cdot 10^{-7}$ | $1.56 \cdot 10^{-26}$ |
| 18 (top) | 0.90 | $\theta_{cos}^{(0,\pi/2)}(u)$ | $10^{-4}$ | $10^{-4}$ | $10^{-3}$ | 40.2 | 200 | $6.10 \cdot 10^{-6}$ | $2.04 \cdot 10^{-26}$ |
| 18 (bot) | 0.95 | $\theta_C = \pi/4$ | $10^{-4}$ | $10^{-4}$ | $5 \cdot 10^{-3}$ | 40.4 | 200 | $9.70 \cdot 10^{-6}$ | $8.70 \cdot 10^{-27}$ |
| 19 (top-left) | 0.80 | $\theta_0^{5\pi/12}(u)$ | $10^{-4}$ | $10^{-4}$ | 0 | 19.2 | 150 | $2.26 \cdot 10^{-8}$ | $1.51 \cdot 10^{-23}$ |
| 19 (top-right) | 0.80 | $\theta_0^{\pi/3}(v)$ | $10^{-4}$ | $10^{-4}$ | 0 | 22.0 | 150 | $2.63 \cdot 10^{-8}$ | $2.37 \cdot 10^{-26}$ |
| 19 (bot-left) | 0.80 | $\theta_{cos}^{(0,\pi/2)}(u)$ | $10^{-4}$ | $10^{-4}$ | 0 | 13.6 | 150 | $1.98 \cdot 10^{-8}$ | $8.23 \cdot 10^{-28}$ |
| 19 (bot-right) | 0.80 | $\theta_{cos}^{(0,\pi/2)}(v)$ | $10^{-5}$ | $10^{-5}$ | 0 | 15.6 | 150 | $5.22 \cdot 10^{-8}$ | $1.99 \cdot 10^{-24}$ |

**Table 2**
Summary of parameter initializations, weights, residual, and times used for all our examples. The residual accounts only for the contributions of $E_{\text{oc}}$, $E_{\text{prox}}$, and $E_{\tan}$. As a quality measure of the L-net, we show the residual of $E_{\text{oc}}$ measured after the extra optimization steps. All computations were performed using a Python implementation of our algorithm, running on a MacBook Pro with an Apple M1 chip (8-core CPU, 8-core GPU, and 16-core Neural Engine).

- *Cosine:* along the $u$-direction and $v$-directions, respectively

$$\theta_{\cos}^{(\theta_{min},\,\theta_{max})}(u) = \frac{\theta_{min} + \theta_{max}}{2} + \frac{\theta_{max} - \theta_{min}}{2}\cos(2\pi\, u), \tag{28}$$

$$\theta_{\cos}^{(\theta_{min},\,\theta_{max})}(v) = \frac{\theta_{min} + \theta_{max}}{2} + \frac{\theta_{max} - \theta_{min}}{2}\cos(2\pi\, v). \tag{29}$$

A summary of our results is provided in Table 2. Our method produces a variety of design patterns for a given input surface, where the user can explore different choices of radius and L-conjugate angles (see, for example, Figs. 18

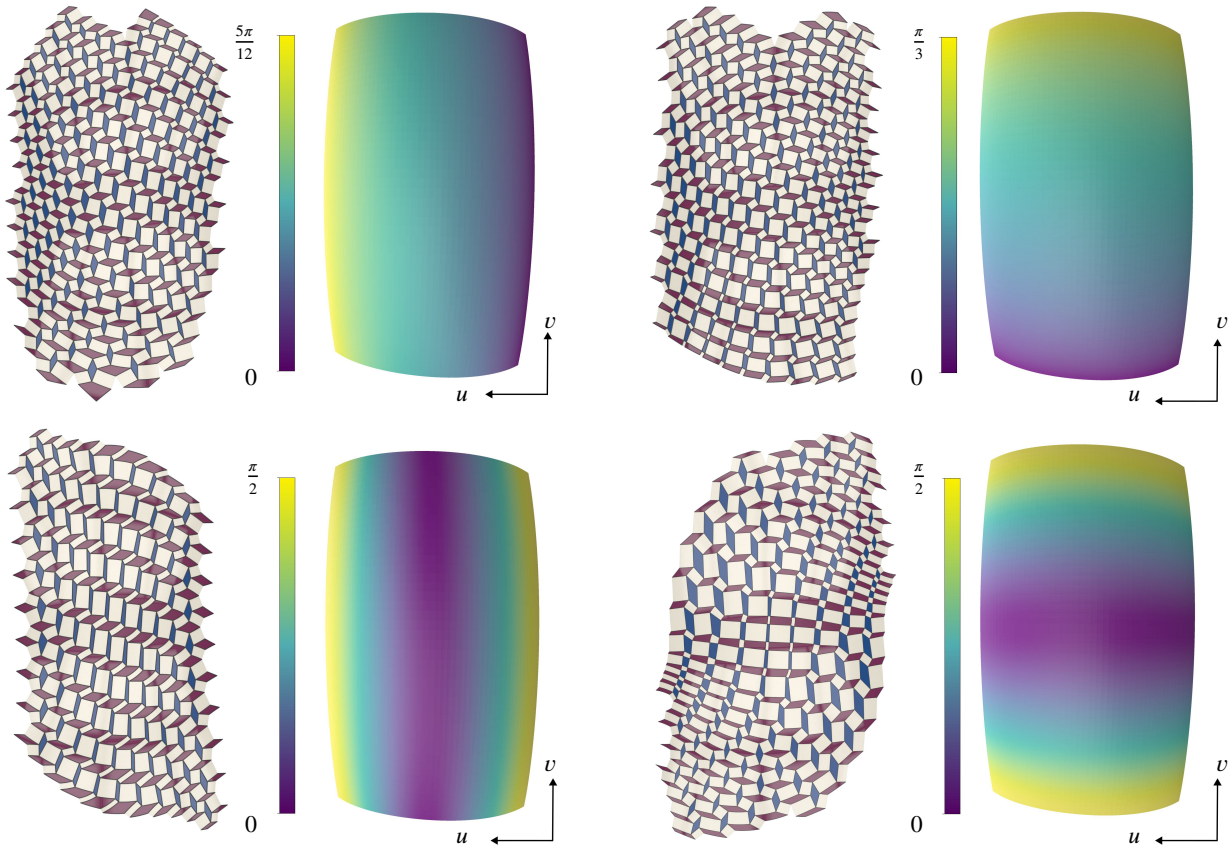


**Figure 19:** L-net patterns obtained from different initialization functions $\theta(u, v)$, which prescribe the angle between the first direction of an L-conjugate pair and the first principal direction at each point $(u, v)$ of the parameter domain. For each pattern, the *right* image shows the scalar field $\theta(u, v)$ visualized on the surface (color scale shown in the color bar). (Top, left to right) $\theta_0^{5\pi/12}(u)$ and $\theta_0^{\pi/3}(v)$; (bottom, left to right) $\theta_{\cos}^{(0,\pi/2)}(u)$ and $\theta_{\cos}^{(0,\pi/2)}(v)$.

and 19). We observe that minimizing $E_{\mathrm{td}}$ has a fairness effect on the sphere center mesh; however, it also tends to shrink the L-net globally, as shown in Fig. 17, and the overall improvement in spherical panel size is minimal. We also observe that, in general, larger spherical panels are obtained when the radius $r$ is chosen close to the smallest principal curvature radius. However, the L-conjugate directions also influence the final panel shapes, as seen in Fig. 19, where despite using the same sphere congruence relatively close to the smallest principal curvature spheres, the resulting spherical panels exhibit considerable size variation. Similarly, Fig. 3 illustrates this effect, where smaller spherical panels appear in the narrow regions of the spiral design and larger ones in the wider regions. This indicates that obtaining larger panels likely has to be addressed prior to the choice of the conjugate frame field and requires further exploration.

*Conclusion and future work* We have introduced the new concept of L-conjugate parameterizations of a surface with respect to an attached sphere congruence. Based on this theoretical framework, we devised an algorithm for the approximation of positively curved surfaces by L-nets. These are smooth surfaces formed by quadrilateral planar, conical, and spherical patches.

We are currently working on the Möbius geometric counterpart, namely the approximation of a surface $f$ by a quad mesh with spherical faces and circular edges so that the spheres are close to those of an attached sphere congruence. This is related to another concept of conjugacy, which possesses similarly nice properties as L-conjugacy.

The sphere geometries of Möbius and Laguerre are sub-geometries of Lie sphere geometry, which would be another direction for future work. Special cases of the corresponding Lie geometric meshes can be obtained by applying

Möbius transformations to L-nets. This removes the restriction to positively curved surfaces. The resulting surfaces are composed of spherical patches and patches of Dupin cyclides, arranged in a checkerboard pattern. The cyclides are the images of the cones under Möbius transformations. The resulting surfaces have more degrees of freedom than the cyclidic nets, which are principal curvature parameterizations that consist of smoothly joined cyclide patches (Bo, Pottmann, Kilian, Wang and Wallner, 2011; Bobenko and Huhnen-Venedey, 2012).

Another interesting direction is the application of analogs (of Minkowski lifts) of our L-nets in 4-dimensional *simply isotropic space* with the metric of signature $(+,+,+,0)$. These are lifts of ordinary conjugate nets in $\mathbb{R}^3$ to 4-dimensional space. We can then use them to initialize optimization towards L-nets in $\mathbb{R}^{3,1}$ by gradually changing the metric. Such a general approach has been proved successful for a class of *Euclidean* problems, for instance, the construction of asymptotic nets with a constant node angle, as demonstrated in a recent series of papers (Skopenkov and Yorov, 2025; Yorov, Skopenkov and Pottmann, 2025a; Yorov, Wang, Skopenkov, Pottmann and Jiang, 2025b), where the last one serves as an introduction to this approach and summarizes the achievements. Having an application to *Minkowskian* geometry is of additional interest.

## References


Affolter, N.C., Dellinger, F., Müller, C., Polly, D., Smeenk, N., 2024. Discrete Lorentz surfaces and s-embeddings ii: maximal surfaces. arXiv:2411.19055.

Affolter, N.C., Dellinger, F., Müller, C., Polly, D., Smeenk, N., 2025. Discrete Lorentz surfaces and s-embeddings i: isothermic surfaces. Journal of Geometry and Physics 213, 105482. URL: https://www.sciencedirect.com/science/article/pii/S039304402500066X, doi:10.1016/j.geomphys.2025.105482.

Affolter, N.C., Techter, J., 2026. Principal binets. Discrete & Computational Geometry. doi:10.1007/s00454-025-00807-5.

Blaschke, W., 1929. Vorlesungen über Differentialgeometrie und geometrische Grundlagen von Einsteins Relativitätstheorie. Band III. Differentialgeometrie der Kreise und Kugeln. Springer, Berlin.

Blaschke, W., Leichtweiß, K., 1973. Elementare Differentialgeometrie. Springer, Berlin-New York. Fünfte vollständig neubearbeitete Auflage von K. Leichtweiß , Die Grundlehren der mathematischen Wissenschaften, Band 1.

Bo, P., Pottmann, H., Kilian, M., Wang, W., Wallner, J., 2011. Circular arc structures. ACM Trans. Graph. 30, 101:1–101:11. doi:10.1145/2010324.1964996.

Bobenko, A.I., Huhnen-Venedey, E., 2012. Curvature line parametrized surfaces and orthogonal coordinate systems: discretization with Dupin cyclides. Geom. Dedicata 159, 207–237. doi:10.1007/s10711-011-9653-5.

Bobenko, A.I., Lutz, C.O.R., Pottmann, H., Techter, J., 2021. Non-Euclidean Laguerre geometry and incircular nets. Springer Briefs in Mathematics. doi:10.1007/978-3-030-81847-0.

Bobenko, A.I., Schröder, P., 2005. Discrete Willmore flow, in: Proc. Eurographics Symposium on Geometry Processing, Eurographics Assoc.. pp. 101–110. doi:10.1145/1198555.1198664.

Bobenko, A.I., Suris, Y.B., 2006. Isothermic surfaces in sphere geometries as Moutard nets. Proceedings of The Royal Society A Mathematical Physical and Engineering Sciences 463, 3171–3193. doi:10.1098/rspa.2007.1902.

Bobenko, A.I., Suris, Y.B., 2007. On organizing principles of discrete differential geometry. geometry of spheres. Russian Mathematical Surveys 62, 1–43. doi:10.1070/RM2007v062n01ABEH004380.

Bobenko, A.I., Suris, Y.B., 2008. Discrete differential geometry. Integrable structure. volume 98 of *Graduate Studies in Mathematics*. American Mathematical Society. doi:10.1007/978-3-7643-8621-4.

Cecil, T.E., 2008. Lie sphere geometry. Springer. doi:10.1007/978-0-387-74656-2.

Dellinger, F., 2024. Discrete isothermic nets based on checkerboard patterns. Discrete & Computational Geometry 72, 209–245. doi:10.1007/s00454-023-00558-1.

Ebke, H.C., Bommes, D., Campen, M., Kobbelt, L., 2013. QEx: Robust quad mesh extraction. ACM Trans. Graph. 32, 168:1–168:10. URL: http://doi.acm.org/10.1145/2508363.2508372, doi:10.1145/2508363.2508372.

Eigensatz, M., Kilian, M., Schiftner, A., Mitra, N.J., Pottmann, H., Pauly, M., 2010. Paneling architectural freeform surfaces. ACM Trans. Graph. 29, 45:1–45:10. doi:10.1145/1778765.1778782.

Gavriil, K., Schiftner, A., Pottmann, H., 2019. Optimizing B-spline surfaces for developability and paneling architectural freeform surfaces. Computer-Aided Design 111, 29–43. doi:10.1016/j.cad.2019.01.006.

Hertrich-Jeromin, U., 2003. Introduction to Möbius Differential Geometry. Cambridge University Press. doi:10.1017/CBO9780511546693.

Jacobson, A., Panozzo, D., et al., 2018. libigl: A simple C++ geometry processing library. Https://libigl.github.io/.

Jadon, E., Thomaszewski, B., Apolinarska, A.A., Poranne, R., 2022. Continuous deformation based panelization for design rationalization. ACM Trans. Graph. doi:10.1145/3550469.3555414.

Kilian, M., Ramos-Cisneros, A., Müller, C., Pottmann, H., 2023. Meshes with spherical faces. ACM Trans. Graph. 42, 177:1–177:19. doi:10.1145/3618345.

Liu, Y., Pottmann, H., Wallner, J., Yang, Y.L., Wang, W., 2006. Geometric modeling with conical meshes and developable surfaces. ACM Trans. Graph. 25, 681–689. doi:10.1145/1179352.1141941.

Liu, Y., Xu, W., Wang, J., Zhu, L., Guo, B., Chen, F., Wang, G., 2011. General planar quadrilateral mesh design using conjugate direction field. ACM Trans. Graph. 30, 140, 1–10. doi:10.1145/2024156.2024174. proc. SIGGRAPH Asia.

Marquardt, D.W., 1963. An algorithm for least-squares estimation of nonlinear parameters. Journal of the Society for Industrial and Applied Mathematics 11, 431–441. doi:10.1137/0111030.

Musso, E., Nicolodi, L., 2018. Surfaces in Laguerre geometry. Banach Center Publications 117 (2019), 223-255 117, 223–255. doi:10.4064/bc117-8, arXiv:1802.05507.

Pellis, D., Wang, H., Kilian, M., Rist, F., Pottmann, H., Müller, C., 2020. Principal symmetric meshes. ACM Trans. Graph. 39, 127:1–127:17. doi:10.1145/3386569.3392446.

Peng, C.H., Jiang, C., Wonka, P., Pottmann, H., 2019. Checkerboard patterns with black rectangles. doi:10.1145/3355089.3356514.

Peternell, M., Pottmann, H., 1998. A Laguerre geometric approach to rational offsets. Comput. Aided Geom. Design 15, 223–249. doi:10.1016/S0167-8396(97)00024-1.

Pottmann, H., Eigensatz, M., Vaxman, A., Wallner, J., 2015. Architectural geometry. Computers and Graphics 47, 145–164. doi:10.1016/j.cag.2014.11.002.

Pottmann, H., Grohs, P., Mitra, N.J., 2009. Laguerre minimal surfaces, isotropic geometry and linear elasticity. Adv. Comp. Math 31, 391–419. doi:10.1007/s10444-008-9076-5.

Pottmann, H., Peternell, M., 1998. Applications of Laguerre geometry in CAGD. Computer Aided Geometric Design 15, 165–186. doi:10.1016/S0167-8396(97)00023-X.

Ramos-Cisneros, A., Aikyn, A., Kilian, M., Pottmann, H., Müller, C., 2024. Approximation by meshes with spherical faces. ACM Trans. Graphics 43, 179:1–179:17. doi:10.1145/3687942.

Skopenkov, M., Bo, P., Bartoň, M., Pottmann, H., 2020. Characterizing envelopes of moving rotational cones and applications in cnc machining. Comp. Aided Geometric Design 83, 101944. doi:10.1016/j.cagd.2020.101944.

Skopenkov, M., Pottmann, H., Grohs, P., 2012. Ruled Laguerre minimal surfaces. Math. Zeitschrift 272, 645–674. doi:10.1007/s00209-011-0953-0.

Skopenkov, M., Yorov, K., 2025. Families of surfaces with constant ratio of principal curvatures and plateau's problem. arXiv:2510.14527.

Tao, J., Yang, Y.L., Deng, B., 2025. Learning conjugate direction fields for planar quadrilateral mesh generation. arXiv:2511.11865.

Thiery, J.M., Guy, E., Boubekeur, T., 2013. Sphere-meshes: Shape approximation using spherical quadric error metrics. ACM Trans. Graph. 32, 178:1–178:12. doi:10.1145/2508363.2508384.

Thiery, J.M., Guy, E., Boubekeur, T., Eisemann, E., 2016. Animated mesh approximation with sphere-meshes. ACM Trans. Graph. 35, 30:1–30:13. doi:10.1145/2898350.

Tkach, A., Pauly, M., Tagliasacchi, A., 2016. Sphere-meshes for real-time hand modeling and tracking. ACM Trans. Graph. 35, 222:1–222:11. doi:10.1145/2980179.2980226.

Yorov, K., Skopenkov, M., Pottmann, H., 2025a. Surfaces of constant principal-curvatures ratio in isotropic geometry. Contrib. Algebra Geom. 66, 775–814. doi:10.1007/s13366-024-00768-5.

Yorov, K., Wang, B., Skopenkov, M., Pottmann, H., Jiang, C., 2025b. Solving euclidean problems by isotropic initialization. arXiv:2506.01726.

Zadravec, M., Schiftner, A., Wallner, J., 2010. Designing quad-dominant meshes with planar faces. Comput. Graph. Forum 29, 1671–1679. doi:10.1111/j.1467-8659.2010.01776.x. proc. SGP.

## CRediT authorship contribution statement

**Anthony Ramos-Cisneros:** Writing - Original Draft, Investigation, Conceptualization, Methodology, Software, Visualization, Writing - Review & Editing. **Mikhail Skopenkov:** Writing - Review & Editing, Formal Analysis. **Helmut Pottmann:** Writing - Original draft preparation, Investigation, Formal Analysis, Conceptualization, Writing - Review & Editing, Supervision.

## Funding

This research has been supported by King Abdullah University of Science and Technology baseline funding.

## Data availability

Data sharing is not applicable to this article, as no datasets were generated or analyzed during the current study.

## Declaration of competing interest

The authors declare that they have no known competing financial interests or personal relationships that could have appeared to influence the work reported in this paper